HUMAN-LIKE EPISODIC MEMORY
FOR INFINITE CONTEXT LLMS

Zafeirios Fountas[1], **Martin A Benfeghoul**[1,*], **Adnan Oomerjee**[1,*], **Fenia Christopoulou**[1],
Gerasimos Lampouras[1], **Haitham Bou-Ammar**[1,2] **and Jun Wang**[2]

[1]Huawei Noah's Ark Lab, London, UK
[2]University College London, UK
{zafeirios.fountas,adnan.ebrahim.oomerjee,efstathia.christopoulou}@huawei.com
{gerasimos.lampouras,haitham.ammar}@huawei.com
martin.antoine.benfeghoul@h-partners.com
jun.wang@ucl.ac.uk

ABSTRACT

Large language models (LLMs) have shown remarkable capabilities, but still struggle with processing extensive contexts, limiting their ability to maintain coherence and accuracy over long sequences. In contrast, the human brain excels at organising and retrieving episodic experiences across vast temporal scales, spanning a lifetime. In this work, we introduce EM-LLM, a novel approach that integrates key aspects of human episodic memory and event cognition into LLMs with no fine-tuning, enabling them to handle practically infinite context lengths while maintaining computational efficiency. EM-LLM organises sequences of tokens into coherent episodic events using a combination of Bayesian surprise and graph-theoretic boundary refinement in an online fashion. When needed, these events are retrieved through a two-stage memory process, combining similarity-based and temporally contiguous retrieval for efficient and human-like access to relevant information. Experiments on the LongBench and ∞-Bench benchmarks demonstrate EM-LLM's superior performance, consistently outperforming the state-of-the-art retrieval model InfLLM across various baseline LLMs. In addition, EM-LLM outperforms its popular counterpart, RAG, in a wide range of tasks, while requiring similar resources. Notably, EM-LLM's performance even surpasses full-context models in most tasks, while successfully performing retrieval across 10 million tokens – a scale computationally infeasible for such models. Finally, our analysis reveals strong correlations between EM-LLM's event segmentation and human-perceived events, suggesting a bridge between this artificial system and its biological counterpart, thereby offering a novel computational framework for exploring human memory mechanisms.

1 INTRODUCTION

For contemporary pre-trained large language models (LLMs), the context window serves as the primary mechanism to incorporate domain-specific, private, or common up-to-date information. However, despite their remarkable and ever-expanding capabilities, LLMs still exhibit significant limitations when tasked with processing extensive contexts (Liu et al., 2024a). These limitations stem from inherent challenges in Transformer-based architectures. Recent studies have shown that Transformers struggle with extrapolating to contexts longer than their training window size (Kazemnejad et al., 2024). On top of this, employing softmax attention over extended token sequences requires substantial computational resources for each token generation, while the resulting aggregated embeddings (the weighted sums of value vectors) risk becoming excessively noisy and losing their distinctiveness (Tworkowski et al., 2023).

To mitigate these challenges, recent works have focused on retrieval-based methods, either in the form of in-context augmentation (e.g., retrieval-augmented generation (RAG)-based techniques (Lewis

---

*Equal Contribution.

et al., 2020; Gao et al., 2024)) or via retrieval of previously-inferred key-value pairs (KV) within individual attention heads (Wu et al., 2022; Tworkowski et al., 2023; Bertsch et al., 2023). Notably, state-of-the-art (SOTA) performance is achieved when KV pairs are initially organised into non-overlapping segments and then retrieved together as one block of sequential tokens (Xiao et al., 2024a). While such techniques present interesting research avenues, we still see a significant gap between the performance of LLMs in short- vs long-context tasks, even when existing long-context architectures are employed (Liu et al., 2024a).

This work tackles the above challenges and attempts to bridge this performance gap by taking inspiration from the algorithmic interpretation of *episodic memory in the human brain* – the memory system responsible for encoding, storing, and retrieving personal experiences and events. The brain makes sense of its continuous experience in the real world by segmenting it into discrete episodic events (Clewett et al., 2019; Zacks, 2020), which are first organised in a hierarchical and nested-timescale structure (Baldassano et al., 2017) and then stored in long-term memory. Notably, the boundaries between such events are the access points for memory retrieval (Michelmann et al., 2023a) and are widely believed to correspond to points in time with high prediction errors between the brain's generative model and its raw sensory input (a.k.a., *surprise*). In this context, surprise refers to moments when the brain's predictions about incoming sensory information are significantly violated, leading to a mismatch between what is expected and what is actually perceived. These instances of high surprise are thought to signal important changes in the environment or narrative, prompting the brain to segment the ongoing experience into distinct events (Zacks et al., 2007; 2011; Roseboom et al., 2019; Sinclair et al., 2021; Fountas et al., 2022). Once segmented and stored, the brain re-

Figure 1: **Top:** EM-LLM$_S$ vs. RAG (NV-Embed-v2 retriever) vs. full-context, with LLaMA-3.1-8B as the base LLM, evaluated on LongBench. **Bottom:** Comparison of various long-sequence methods (sorted based on their context window length) on an extended version of ∞-Bench's *Retrieve.PassKey*. Baseline data taken from Ding et al. (2024).

calls episodic memories based on their similarity to current experience, recency, original temporal order, and their proximity to other recalled memories (temporal asymmetry and contiguity (Howard and Kahana, 2002)).

Following these insights, we propose a novel architecture, *EM-LLM*, which integrates crucial aspects of event cognition and episodic memory into Transformer-based LLMs. For memory formation, we segment the sequence of tokens presented to the underlying LLM into individual memory units representing episodic events. The boundaries, and thus the size of those events, are initially determined dynamically, based on the level of surprise of the model during inference, and then refined to maximise cohesion within memory units and separation of memory content across them (see Section 3.2). This refinement process leverages graph-theoretic metrics, treating the similarity between attention keys (the learned representations used in Transformer self-attention mechanisms) as a weighted adjacency matrix, and aims to enhance the model's ability to efficiently recall relevant information when addressing complex tasks with extended contexts. Importantly, this memory formation process incurs minimal additional computational cost. The surprise-based segmentation requires no extra computation and the refinement step has a complexity of $\mathcal{O}(kn)$, where k is typically very small compared to the number of tokens n. With this efficient memory formation process, by grouping similar information in single units, we minimise the number of units needed to recall details around specific events. For memory recall, our approach integrates similarity-based retrieval with
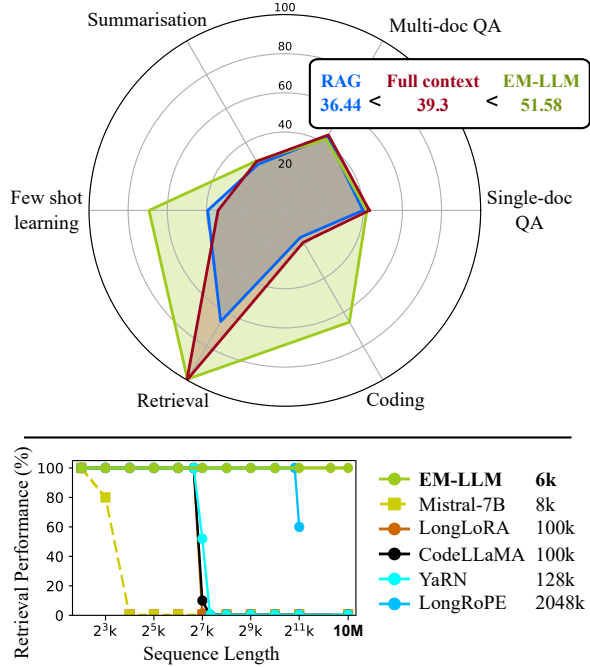
mechanisms that facilitate temporal contiguity and asymmetry effects. By retrieving and buffering salient memory units, our model leverages and enhances the recently discovered propensity of LLMs to exhibit human-like patterns in sequential information retrieval (Ji-An et al., 2024). This method not only ensures efficient access to pertinent information but also mimics the temporal dynamics found in human free recall studies (such as Howard and Kahana (2002)), further enhancing the model's ability to handle complex tasks that require nuanced temporal reasoning.

In this work, we show that our method is scalable and significantly outperforms the SOTA retrieval model InfLLM (Xiao et al., 2024a), as well as RAG and full-context methods, on the widely-used LongBench (Bai et al., 2023) and ∞-Bench (Zhang et al., 2024) benchmarks designed for long-context tasks (see Fig. 1). Furthermore, we perform successful passkey retrieval across 10M tokens, a length which is computationally infeasible for current full-context models. To further prove our hypotheses, we then employ a series of human-annotated podcast scripts to show that information in LLM attention heads can be semantically grouped in a way that correlates with the event structure perceived by humans. Therefore, LLM-perceived surprise can indeed serve as a proxy for the cognitive signals that drive human event segmentation, as confirmed by previous studies (Kumar et al., 2023). Finally, using the long-context PG-19 dataset (Rae et al., 2020), which comprises a diverse corpus of English books, we evaluate the effectiveness of our segmentation method for grouping relevant information and assess the performance of different boundary refinement objectives.

2 RELATED WORK

2.1 LONG-CONTEXT IN LLMS

Recently, several approaches have been proposed to extend the context window of Transformer-based models. These include methods that address the limited representational capacity of softmax attention, and its quadratic computational and memory cost (Katharopoulos et al., 2020; Munkhdalai et al., 2024). Other methods target the poor extrapolation of typical positional encodings to out-of-distribution context lengths (Kazemnejad et al., 2024). The latter is evident in most widely used methods, including the original absolute positional encodings (Vaswani et al., 2017) and the more recent relative positional encodings, such as the popular Rotary Positional Embeddings (RoPE) (Su et al., 2024). To address this, some approaches propose scaling of the rotation angles (Chen et al., 2024a) or the base constant (Xiong et al., 2023; Liu et al., 2024b; Peng et al., 2024; Ding et al., 2024). Others, scale positions without affecting the embedding function (Press et al., 2021; Chen et al., 2023; Jin et al., 2024), explore alternative strategies such as KERPLE (Chi et al., 2022) and FIRE (Li et al., 2024a) or adopt relative position embedding mechanisms from certain LMs like T5 (Raffel et al., 2020).

Concerning computational efficiency and diluted attention, successful approaches propose methods for general improvements to Transformer efficiency through optimised computations (Dao, 2024; Han et al., 2024a; Aminabadi et al., 2022; Kwon et al., 2023; Liu et al., 2024c; Brandon et al., 2023) or compression techniques (Nawrot et al., 2024; Zhang et al., 2023), as well as training methods tailored for long-context scenarios (Zhu et al., 2024; Chen et al., 2024b). Another direction is the utilisation of retrieval-based methods, the vast majority of which relies on a vector database that keeps a key-value cache and scalable approximations of k-nearest neighbors (k-NNs) to perform lookups (Wu et al., 2022; Tworkowski et al., 2023; Bertsch et al., 2023). Interestingly, since using a key-value cache with k-NN lookup can be seen as an approximation of applying softmax attention to the full token sequence (see Appendix E.1), k-NN retrieval methods can be used without fine-tuning (Bertsch et al., 2023). For an exception that does not rely on k-NNs, see Wang et al. (2023).

A recent and interesting variant of k-NN retrieval involves retrieving large groups of tokens, rather than individual ones. Models that rely on this approach include SLED (Ivgi et al., 2023) and the more recent InfLLM (Xiao et al., 2024a), which achieves SOTA performance on long-context benchmarks. InfLLM segments the entire context length into fixed-size memory units and employs k-NN lookup using the tokens with the highest accumulated scores per unit. This can be seen as a form of hierarchical attention, as illustrated in Fig. 2. While group-based retrieval represents a promising direction, our approach significantly advances this concept by dynamically determining token groupings in a manner akin to human memory formation. This effectively addresses a fundamental limitation of InfLLM's fixed-size segmentation and enables more adaptive and context-sensitive processing of extended information.
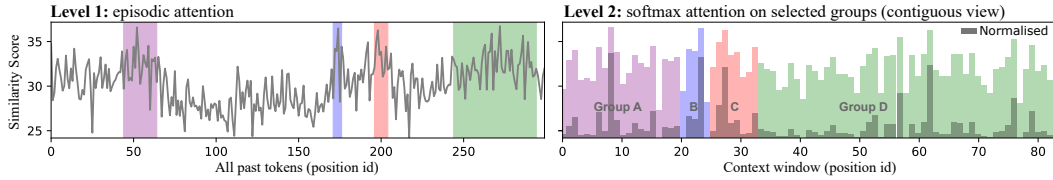
Figure 2: Group-based k-NN retrieval can be seen as a form of hierarchical episodic attention. Initially, $k = 4$ groups of tokens are selected (left) and then used for softmax attention (right), as if all other similarity scores were forced to be zero (non-shaded areas of the left curve). This framework can support multiple levels of episodic attention.

2.2 NEURAL MODELS OF EPISODIC MEMORY AND EVENT COGNITION

The concept of episodic memory, central to our approach, has been extensively studied in both theoretical neuroscience and machine learning. Neural models of episodic memory capture human behaviour and neuroimaging data, providing insights into how the brain processes and stores experiences and suggesting links between memory, efficient representations and navigation of physical and conceptual spaces (Gershman et al., 2012; Benna and Fusi, 2021). In machine learning, episodic memory-inspired approaches have yielded significant improvements across various domains. For instance, episodic control has enhanced reinforcement learning agents' performance and learning speed (Blundell et al., 2016; Pritzel et al., 2017; Coda-Forno et al., 2024). In addition, models of memory construction and consolidation have been successful in alleviating catastrophic forgetting in neural networks (Kirkpatrick et al., 2017; Lopez-Paz and Ranzato, 2017; Chaudhry et al., 2019; Buzzega et al., 2020; Prabhu et al., 2020), including LLMs (Das et al., 2024), and appear to explain key features of human memory, such as imagination and future thinking (Spens and Burgess, 2024).

These models have revealed key aspects of episodic memory, particularly in describing how experiences are segmented into events, and when new memories are encoded and retrieved (Lu et al., 2022). Surprise plays a critical role in this process, triggering event boundaries and memory formation (Fountas et al., 2022; Kumar et al., 2023). This event-based structure is deeply intertwined with our perception of time (Roseboom et al., 2019; Sherman et al., 2022), highlighting the interdependence of memory and temporal cognition. This insight has helped generative models for video (Zakharov et al., 2022a;b) and reinforcement learning (Zakharov et al., 2021) to capture temporal dynamics more accurately. In terms of memory retrieval, studies in human free recall have shown a distinctive increased likelihood of retrieving items encoded close together in time (temporal contiguity) and in succession (temporal asymmetry) (see Fig. 3A). Recently, it was shown that attention heads in Transformer-based LLMs that are associated with in-context learning, already exhibit the same dynamic retrieval behaviour (Ji-An et al., 2024) (Fig. 3B) including both contiguity and asymmetry effects. Therefore, Transformers have the inherent ability to act as episodic memory retrieval models, if provided with the right information within their context window. Our work leverages these concepts of surprise-based event segmentation and LLMs' inherent temporal contiguity and asymmetry effects to enable a new generation of Infinite Context-Length LLMs, capable of processing and understanding information over vastly extended timescales.

3 EM-LLM: LLM WITH EPISODIC MEMORY

3.1 ARCHITECTURE

EM-LLM is designed to be applied directly to pre-trained LLMs, enabling them to handle context lengths significantly larger than their original training length. Our architecture, illustrated in Fig. 3C, divides the context into three distinct groups: initial tokens, evicted tokens and local context. This structure, while incorporating insights from recent work on token block retrieval (Xiao et al., 2024a), introduces novel elements inspired by human episodic memory.

The local context represents the most recent tokens, maximising information about the current task, and fits within the typical context window of the underlying LLM. This group utilises full softmax attention and plays a role similar to the focus of attention in cognitive models of working memory, holding the most immediately relevant information for the current task (Cowan, 2001). The evicted tokens typically comprise the majority of past tokens in a long-context scenario, extending far beyond
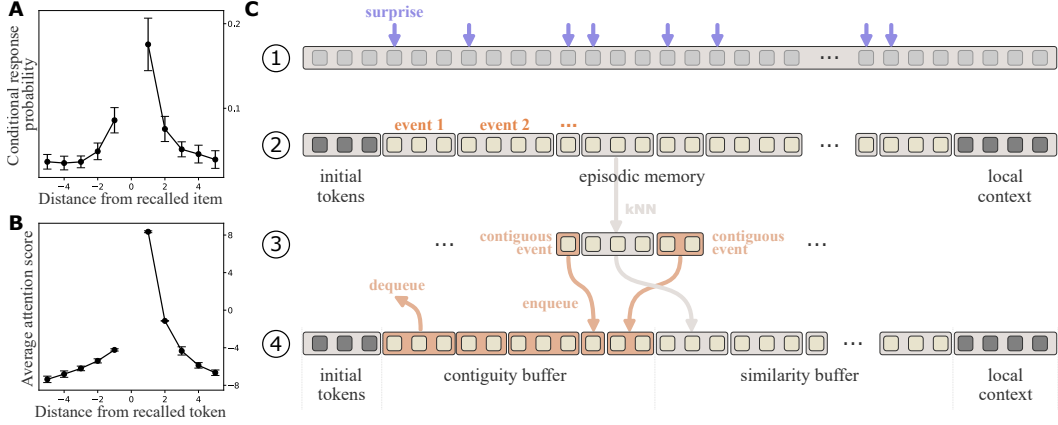
Figure 3: (**A**) Example of the temporal contiguity and asymmetry effect in human free recall. Data averaged over several large free recall studies (adopted from Howard and Kahana (2002)). (**B**) The attention scores of a GPT2 head averaged over all tokens tested (adopted from Ji-An et al. (2024)). (**C**) Schematic illustrating our proposed process for memory formation and retrieval in each layer: ① Input sequence with surprise-based segmentation (purple arrows indicate high surprise). ② Formation of episodic memories: input is segmented into events and stored, with initial tokens and local context preserved. Note that the boundary refinement process is not shown here for clarity. ③ Memory retrieval via k-NN search, selecting contiguous events from episodic memory. ④ Final context window structure, comprising initial tokens, contiguity buffer (populated by neighbouring events), similarity buffer (from k-NN retrieval), and local context.

the LLM's original training length. These tokens are managed by our proposed memory model functioning similarly to short-term episodic memory in the brain. Finally, following previous work, we also maintain a group of 128 initial tokens in the LLM context. These act as *attention sinks* and help recover the performance of window attention, as first observed by Xiao et al. (2024b); Han et al. (2024b) and later adopted by Xiao et al. (2024a). For retrieved tokens, which are therefore discontinuous and outside the local context, we assign a fixed position embedding as in Raffel et al. (2020); Xiao et al. (2024a). This architecture enables EM-LLM to effectively process and utilise information from positions outside its pre-trained local context window, while maintaining the underlying LLM's performance characteristics.

3.2 MEMORY FORMATION VIA SURPRISE

In the context of LLMs, we define episodic memory as the organised, event-based collection of past key-value pairs, analogous to the latent representations of personal experiences in human memory. Just as unexpected or novel information plays a crucial role in human memory formation, we posit that analogous indicators of novelty in LLMs can serve as an effective proxy for identifying significant "events" within the model's experience. In Bayesian terms, surprise is quantified by the negative log-likelihood of observing the current, ground-truth token given the previous tokens in an auto-regressive model, with high values indicating the unpredictability or novelty of each new token within the context according to the model, i.e., being "surprised" by the next token. Following work on cognitive modelling (Roseboom et al., 2019; Fountas et al., 2022), we employ a thresholding mechanism to perform an initial identification of event boundaries (used for the first time in LLMs). Formally, a token x_t is considered a potential boundary if its surprise value exceeds a threshold T:

$$-\log P(x_t|x_1,\ldots,x_{t-1};\theta) > T \quad \text{with} \quad T = \mu_{t-\tau} + \gamma\sigma_{t-\tau} \tag{1}$$

where $\mu_{t-\tau:t}$ and $\sigma^2_{t-\tau:t}$ are the mean and variance of surprise for a window offset τ, and γ is a scaling factor. The choice of threshold T is critical in balancing the granularity of segmentation with the model's sensitivity to contextual shifts. If the T is too high, we will identify very few event boundaries, especially if the local context contains few surprising tokens. Conversely, a low T results in frequent boundary identification. Using a moving window ensures that T adapts to contextual shifts, minimizing the need for manual tuning while maintaining control over threshold sensitivity via γ. This initial segmentation results in a set of potential event boundaries $\mathcal{B} = b_1, b_2, ..., b_k$, where

Algorithm 1 Event segmentation in KV cache

Input: tok: List of tokens in the sequence
Input: T: Threshold for surprisal to identify initial boundaries
Input: f: Metric function to evaluate potential boundaries
Output: $\mathcal{B}$: List of final boundary positions
1: $\mathcal{B} \leftarrow$ [i for i in range(`length(tok)`) if $-\log(P(\texttt{tok}[i])) > T$]   ▷ Boundary identification
2: **for** i in range(length($\mathcal{B}$)) **do**
3:      $\alpha, \beta = \mathcal{B}[i], \mathcal{B}[i+1]$
4:      $\mathcal{B}[i+1] \leftarrow \arg\max_{\hat{\beta} \in (\alpha, \beta]} f(A, \{\alpha, \hat{\beta}\})$ ▷ Boundary refinement
5: **end for**
6: **return** $\mathcal{B}$

---

each b_i represents the index of a token exceeding the surprise threshold. These boundaries serve as the starting point for our subsequent refinement process, which aims to optimise the intra-event coherence and inter-event distinctiveness of the resulting memory segments.

3.3 BOUNDARY REFINEMENT

While surprise-based segmentation provides an effective initial estimate of event boundaries, we make the key observation that the utility of elements within an event, during memory recall, depends on their likelihood of being utilised by the current query. Therefore, we theorise that memory recall will be most efficient with high intra-event similarity between keys while maintaining low inter-event similarity. For instance, see the similarity of groups in Fig. 2. To further ensure this, we introduce a boundary refinement step that looks to optimise this objective. Such an objective is typically optimised in the context of graph-clustering, hence we express this refinement process in a graph-theoretic manner. To achieve this, we treat the similarity matrix between all keys of an attention head h within the local context window for tokens $x_1, x_2, ..., x_n$ as an adjacency matrix. We define the adjacency matrix A^h as

$$A_{ij}^h = \text{sim}(K_i^h, K_j^h), \tag{2}$$

where K_i^h and K_j^h are the key vectors corresponding to tokens x_i and x_j, respectively. The similarity function measures the closeness of two key vectors; in our implementation, we use dot product similarity ${K^h}_i^{\mathsf{T}} \cdot K_j^h$ due to its effectiveness in capturing semantic relationships in high-dimensional spaces (Vaswani et al., 2017) and to align with the mechanism of self-attention in Transformers.

To evaluate the quality of potential boundaries, we define a metric function $f(A, \mathcal{B}) : \mathbb{R}^{n \times n} \times \{1, \ldots, n\}^k \rightarrow \mathbb{R}$. This function quantifies the cohesion within events and separation between events based on the graph structure represented by the similarity matrix A and event boundaries $\mathcal{B}$. We experiment with two widely-accepted graph-clustering metrics: *modularity* and *conductance* (Miasnikof et al., 2018). Modularity (Newman and Girvan, 2004) provides a measure of the quality of a particular division of a network into communities, with higher values indicating higher edge density in the identified cluster when compared to the density of edges expected in a random cluster. As our edge weights represent the similarity between two tokens, we seek to maximise this metric. Modularity is defined as:

$$f_M(A^h, \mathcal{B}) = \frac{1}{4m} \sum_{i,j} \left[A_{ij}^h - \frac{\sum_i A_{ij}^h \cdot \sum_j A_{ij}^h}{2m} \right] \delta(c_i, c_j) \tag{3}$$

where m is the total edge weight in the graph, c_i is the community (episodic event) to which node i is assigned, and δ is the Kronecker delta function. Conductance, on the other hand, measures the fraction of total weighted edges cut by a given community boundary, and is defined as:

$$f_C(A^h, \mathcal{B}) = \min_{S \in V} \frac{\sum_{i \in S, j \notin S} A_{ij}^h}{\min(\text{vol}(S), \text{vol}(V \setminus S))}, \quad \text{with vol}(S) = \sum_{i,j \in S} A_{ij}, \text{ vol}(V \setminus S) = \sum_{i,j \notin S} A_{ij} \tag{4}$$

where $S = \{b_i, b_i + 1, ..., b_{i+1}\}$ is a subset of all nodes $V = \{b_1, b_1 + 1, ..., b_k\}$ in the induced graph, with $b_i \in \mathcal{B}$. Lower conductance values indicate better community structure. Our boundary refinement algorithm iteratively adjusts the initial surprise-based boundaries to optimise these metric

functions. While our best results are achieved using modularity, we also include comparisons with conductance-based boundary refinement to provide a comprehensive analysis. The overall process is summarized in Algorithm 1.

This algorithm first identifies initial boundaries based on the surprise threshold T, then refines these boundaries by finding the optimal position $\hat{\beta}$ between each pair of consecutive initial boundaries (α, β) that optimises the chosen metric function f (either maximising modularity or minimising conductance). This process ensures that the final segmentation (1) captures points of high surprise and (2) optimises for coherent information grouping. The boundary identification step incurs negligible computational cost, as it only evaluates existing LLM outputs. The time complexity of Algorithm 1 is dominated by the boundary refinement step, which has an overall complexity of $\mathcal{O}(kn)$, where k is the number of initial boundaries and n is the sequence length (for details see Appendix C.1).

3.4 MEMORY RETRIEVAL

When inferring a new token, a number of episodic events are selected and become a part of the (extended) context window of the underlying LLM. Our memory retrieval process employs a two-stage mechanism to select relevant episodic events for the LLM's context window (Fig. 3C). First, we retrieve k_s events using k-NN search based on dot product similarity between the current query and representative tokens of each event. These representatives, selected as per Xiao et al. (2024a), are the most influential tokens within each event. For large memory stores, we utilise approximate k-NN (Douze et al., 2024) to maintain efficiency. These k_s events, retrieved based on their similarity to the current query, form a part of the LLM's context window that we refer to as the *similarity buffer*.

The second stage of our retrieval process introduces another buffer, which we refer to as the *contiguity buffer*, designed to maintain temporal context. Implemented as a queue of size k_c, this buffer promotes temporal relationships in retrieval. When an event is retrieved, we also enqueue its neighboring events (within $\pm n$ positions in the original sequence) into this buffer. This mechanism enables the LLM's "induction" attention heads to exhibit the contiguity and asymmetry effects discussed in Section 2.2. The queue structure allows for a natural decay of temporal context as new events are processed, with older or repeated events being dequeued as new ones are added. In total, $k = k_s + k_c$ events are added to the context window, striking a balance between relevance and temporal relationships in a manner analogous to human episodic memory retrieval. Note that each layer retrieves and attends to these k events individually, allowing it to potentially focus on different parts of the context.

4 EXPERIMENTS

4.1 PERFORMANCE OF EM-LLM ON LONG-CONTEXT TASKS

Comparison with KV-retrieval-based LLMs   At the time of writing, InfLLM is considered to be the SOTA KV-retrieval method on long-context benchmarks (LongBench, ∞-Bench), as well as being the only method which uses group-based k-NN retrieval in LLMs on such benchmarks. We, therefore, employ this model as our first baseline for comparison with our own methods.

Results on both benchmarks (Table 1) show that our method is able to improve on InfLLM across 5 different base LLMs, 80% of individual task groups of LongBench and on the overall average. Note that the table shows the best single method in terms of overall performance for each ablation. Looking at individual task performance across all experiments, EM-LLM is able to surpass InfLLM in all tasks (see Appendix A.1). Notably, we see an especially large jump in performance in the retrieval (*Passage*, *KV*, *Passkey*, *Number*) and QA (*Narrative*, *Qasper*, *MultiField*, *Hotpot*, *2Wiki* and *Musique*) tasks across all ablations, with up to a 40% and 29.7% improvement over InfLLM respectively. Such tasks require the model to identify and retrieve specific information within the input sequence, a challenging test for the model's ability to accurately recall a wide range of detailed information from a large context concurrently. This substantial improvement highlights the effectiveness of our event segmentation method in enhancing long-term memory recall and retrieval accuracy in LLMs.

Comparison with RAG and full-context LLMs   To evaluate EM-LLM against prominent methods for handling long contexts, we compared its performance on LLaMA 3.1-8B with two different RAG approaches, including the current SOTA NV-Embed-v2 retriever (Lee et al., 2024), as well as with the brute-force baseline of processing all tokens directly within the LLM's softmax attention (full-context). Across most tasks in our benchmarks, EM-LLM outperformed both RAG and full-

Base LLM	Method	LongBench							∞−Bench					
		SQA	MQA	Sum	FSL	Ret	Cod	**Avg.**	C.D	M.F	MC	R.KV	R.P	R.N
Mistral v2	InfLLM (4k+2k)	**33**	25.5	27.1	66.1	64	54.8	41.9	**29.4**	26.6	**43.2**	95.6	100	99.8
	EM-LLM$_{SM+C}$	32.9	**27**	**27.2**	**66.8**	**84.1**	54.8	**43.7**	28.2	**27.1**	42.8	**99**	100	99.8
LLaMA 3	InfLLM (4k+4k)	38.5	36.9	27	69	84	**53.2**	47	30.5	**23.7**	**43.7**	**5**	100	99
	EM-LLM$_{S}$	**39.3**	**37.7**	**27.0**	**69.2**	**87.5**	50.3	**47.2**	**31.7**	16.9	40.6	4.2	100	**99.5**
LLaMA 3.1	InfLLM (4k+4k)	**41.4**	40.7	29	69	97	**64.2**	51.1	22.6	33.7	46.7	81	100	100
	EM-LLM$_{SM}$	41.2	**41.3**	**29.2**	**69.1**	**98.5**	64.1	**51.3**	22.6	**34**	**47.6**	**90.2**	100	100
Phi 3	InfLLM (1k+3k)	28.4	24.9	25.6	52.9	7.5	57	34.5						
	EM-LLM$_{S}$	**29.2**	**27.1**	**25.9**	**53.5**	**10**	57	**35.4**						
Phi 3.5	InfLLM (1k+3k)	31.7	28.5	23.9	**56.3**	11.5	**40.3**	34.2						
	EM-LLM$_{S}$	**31.8**	**31.9**	**24.5**	55.5	**13**	39.5	**34.9**						

Table 1: EM-LLM performance on LongBench (grouped tasks) and ∞-Bench compared to our baseline InfLLM. **S**: surprise threshold, **SM**: surprise threshold and refinement with modularity, **S+C**: surprise threshold and contiguity buffer, **SM+C**: surprise, refinement and contiguity buffer. Each row indicates the number of local + retrieved tokens (eg. 4k+2k) used for both InfLLM and EM-LLM.

context methods (Fig. 1 and Appendix A.2), exceeding the performance of NV-Embed-v2 by 30.5% on LongBench and by 11.5% on ∞-Bench.

This significant performance boost over RAG can be attributed to EM-LLM's ability to retrieve and incorporate relevant information at each layer individually, rather than relying on a single retrieval step as in RAG (for an illustration, see Supp. Fig. 5). By accessing more specific and contextually relevant information through layer-wise key-value retrieval, EM-LLM effectively addresses RAG's limitations in precision and lower overall performance (Li et al., 2024b). Additionally, EM-LLM's hierarchical attention avoids the issue of diluted attention in large context windows that affects full-context models, enabling it to outperform both RAG and full-context LLMs on the LongBench dataset. Furthermore, EM-LLM demonstrated remarkable scalability by achieving 100% accuracy on the *Passkey.Retrieval* task with sequences up to 5,120k tokens, far beyond the practical limits of full-context LLMs. This highlights EM-LLM's efficiency in handling extremely long contexts, positioning it as a powerful alternative for long-context processing.

4.2 HUMAN AND LLM SURPRISE CLUSTER SIMILAR TOKENS TOGETHER

As mentioned in Section 3.2, we employ modularity and conductance as two refinement objectives in our boundary refinement algorithm, due to their qualities in assessing the intra- and inter-event similarities between individual tokens. We will now use such metrics to compare various event segmentation methods, including human event segmentation data. Additionally, we introduce one further, simple metric for this experiment: the ratio between intra- and inter-community similarity (I/IS), calculated for each head and community S as follows:

$$\text{intra} = \sum_{i \in S, j \in S} A_{ij}, \qquad \text{inter} = \sum_{i \in S, j \notin S} A_{ij}, \qquad \text{I/IS} \equiv \frac{\text{intra}}{\text{inter}} \tag{5}$$

Kumar et al. (2023) found strong correlations between human-perceived events and prediction errors across 3 short podcasts (7-30 minutes on average), when processing the corresponding transcript with an LLM. Taking advantage of such human-annotated data and results from previous studies on this dataset (Michelmann et al., 2021; Lositsky et al., 2016), we compare the segmentation quality and correlation with human segmentation for each of our methods (4) using our similarity metrics.

As shown in Fig. 4A, human-perceived events achieve significantly higher scores in similarity metrics compared to fixed or random events, suggesting that surprise is indeed an important factor for humans in their own perception of events. Furthermore, surprise-only segmentation (**S**) achieves very similar results to humans, while the addition of our refinement algorithm (**SM**, **SC**, **FM**, **FC**) significantly improves performance. Fig. 4B further shows that surprise-based methods (**S**, **SM**, **SC**), consistently identify event boundaries that are closest to those perceived by humans.
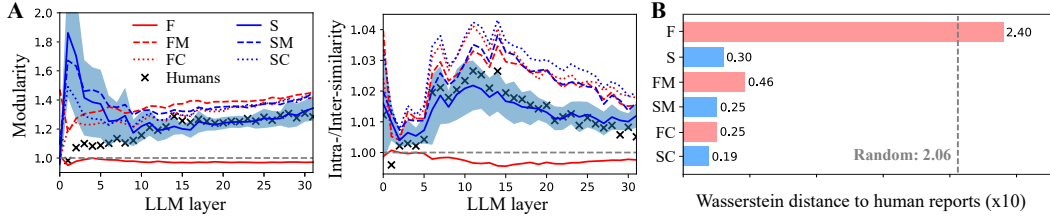
Figure 4: Comparison of human event segmentation with different computational segmentation methods in a human-annotated audio dataset (see also Appendix B). **(A)** Difference in metrics for the cohesion and separation of KV cache of each LLaMA2 layer. The graphs report the difference of each method with the corresponding random segmentation. **(B)** Distance between human reports and different methods. In both sets of results, fixed methods (*F*, *FM*, *FC*) perform worse than their surprise-based counterparts (*S*, *SM*, *SC*) with InfLLM's method (*F*) performing worse than random.

LLM	Metric	F	FM	FC	S	SM	SC
Mistral-7B	Mod ↑	-2.3 ± 4.1	29.2 ± 44.0	6.7 ± 25.9	18.6 ± 29.6	**39.9 ± 55.5**	29.5 ± 42.7
	Con ↓	9.1 ± 8.7	-16.9 ± 6.7	-12.5 ± 9.6	-23.6 ± 9.4	-24.6 ± 9.3	**-27.6 ± 9.8**
	I/IS ↑	-4.3 ± 4.0	31.2 ± 21.4	3.7 ± 14.9	17.9 ± 17.0	**35.3 ± 27.7**	21.6 ± 22.4
LLaMA2-7B	Mod ↑	-1.1 ± 4.3	13.4 ± 19.5	0.6 ± 7.3	8.7 ± 16.0	**18.7 ± 26.4**	11.5 ± 19.4
	Con ↓	11.9 ± 9.8	-18.8 ± 7.4	-13.7 ± 10.9	-29.5 ± 10.2	-29.7 ± 10.1	**-33.3 ± 10.3**
	I/IS ↑	-3.8 ± 3.7	20.7 ± 184.7	-1.1 ± 6.8	15.0 ± 880.0	**25.0 ± 19.9**	16.5 ± 15.4
LLaMA3-8B	Mod ↑	-1.6 ± 3.6	18.9 ± 25.6	0.9 ± 11.8	13.1 ± 21.5	**27.0 ± 35.6**	18.3 ± 28.5
	Con ↓	11.3 ± 9.5	-20.3 ± 6.9	-14.6 ± 11.4	-29.7 ± 9.2	-30.6 ± 9.2	**-33.9 ± 9.6**
	I/IS ↑	-3.8 ± 3.1	24.5 ± 13.9	-1.1 ± 5.8	15.7 ± 11.0	**28.1 ± 16.1**	16.4 ± 12.2

Table 2: Comparison with graph-theoretic metrics in the KV cache of different LLMs and segmentation methods using the PG-19 dataset and $\gamma = 10^{-3}$. Reported values are the difference with random segmentation. Mod: modularity $\times 10^5$, Con: conductance, I/IS: intra/inter-similarity $\times 10^3$.

4.3 COMPARING SEGMENTATION METHODS

Our experiments on the PG-19 dataset (see Table 2) clearly demonstrate that surprise-based segmentation with refinement (**SM**, **SC**) provides the best results in terms of event similarity metrics, regardless of the base LLM used. While the surprise-only method (**S**) achieves decent results, we observe that refinement is especially adept to improving this performance with regards to our metrics, as it is directly optimising for such an objective. Interestingly however, the fixed-based refinement methods (**FM**, **FC**) do not reach the same performance as their surprise-based counterparts, further showing that the initial segmentation with a surprise threshold is crucial to achieving the best possible balance in intra-/inter-similarity with our methods.

4.4 SIMILARITY, CONTIGUITY, RECENCY AND TEMPORAL ORDER

As demonstrated in Tables 1 and 2, along with Fig. 4, each of our ablations show various positive improvements on InfLLM. As mentioned in Section 4.3, refinement has a strong positive impact in improving our similarity metrics. This is seen to translate well to model performance in our experiments, with the addition of refinement achieving the best performance in 60% of tasks across LongBench and ∞-Bench (see Tables 3-7), as well as agreeing with human data (Fig. 4). The effects of contiguity are also clearly demonstrated, with the addition of our contiguity buffer achieving the best performance in 44% of tasks. Furthermore, these methods are seen to be complementary, often improving on both individual additions.

However, the fact that certain tasks still appear to benefit more from either surprise-only, refinement, or contiguity, is an interesting result. This is likely due to the nature of the tasks and the varying importance of contiguity across these tasks. Where contiguity is not crucial, adding such a buffer to our context window also reduces the size of the similarity buffer, and therefore provides potentially less directly relevant events. This is compatible with our own findings that a contiguity buffer that is as big or smaller than the similarity buffer yields the best results (see Fig. 11), suggesting that the similarity buffer is still the most crucial part of our approach. This is especially the case when combined with refinement, which we expect is due to the improved similarity of refined events, hence further reducing the need for contiguous events.

9

5 DISCUSSION

Human studies   Significant correlations have been found between human event segmentation and prediction errors in both LLMs (Kumar et al., 2023) and video models (Fountas et al., 2022; Mariola et al., 2022). Our results add to this growing body of evidence, demonstrating that LLM-based surprise can serve as a proxy for human event segmentation, in multiple levels of hierarchical abstraction, and that the resulting event structure in EM-LLM's attention heads correlates strongly with human-perceived events. This finding creates a more direct, low-level connection between LLM mechanisms and human cognitive processes. Furthermore, our model's use of both similarity-based and temporally contiguous retrieval mechanisms parallels human memory retrieval patterns, allowing for the expression of robust phenomena found in human memory research (Howard and Kahana, 2002). The temporal contiguity effect, where items experienced close together in time are often recalled together, is a robust phenomenon in human memory research (Howard and Kahana, 2002). Further experiments could deepen our understanding of the connections between EM-LLM and human episodic memory. Following Michelmann et al. (2023b), one could test whether the timing of the event boundaries or the degree of modularity per level that our method produces is closer on average to the human consensus, than individual human subjects. Additionally, exploring how different ratios of the contiguity buffer affect the reproduction of human memory biases, and investigating the impact of recency and initial surprise on event recall, could reveal the extent to which EM-LLM exhibits biases found in free recall studies.

Furthermore, EM-LLM's architecture with differentiated context handling (Section 3.1) invites comparisons to cognitive models of human memory beyond episodic. The local context, holding recent and task-relevant information, resembles the limited-capacity working memory system described by Baddeley (2003). Given that EM-LLM's broader context window includes both local context and retrieved memories, it aligns more closely with Ericsson and Kintsch (1995)'s concept of long-term working memory, which allows rapid access to relevant long-term information beyond traditional capacity limits. Alternatively, our architecture parallels Cowan (2001)'s embedded-processes model, where the local context is the "focus of attention", and the full context window represents the activated portion of long-term memory. Future work could explore these analogies further, using EM-LLM as a test-bed for hypotheses about human memory and working memory capacity limits. Inspired by Baddeley's multi-component model, integrating modality-specific buffers into EM-LLM might enhance performance on multi-modal tasks.

Machine learning   In refining event boundaries, we utilised modularity and conductance as metrics for evaluating community structure in the similarity graph of attention keys. While effective in our experiments, we acknowledge that numerous other methods for graph clustering and sequence segmentation could potentially be applied (Fortunato, 2010; Yang et al., 2016). Our choice was motivated by their established theoretical foundations and computational efficiency, though comparative studies suggest performance can vary based on network characteristics (Yang et al., 2016). Interestingly, our surprise-based initial boundary detection shares similarities with Bayesian online change-point detection (Adams and MacKay, 2007), suggesting potential avenues for integrating time series analysis techniques into LLM context processing. Future work could explore whether more sophisticated segmentation or clustering algorithms could improve EM-LLM's performance, particularly for extremely long contexts or streaming data scenarios. Such investigations could enhance our model and contribute to understanding how information is structured and processed in LLMs, bridging the gap between traditional sequence analysis and LLM context processing.

Looking ahead, promising directions for future research include extending our segmentation processes to operate at each layer of the Transformer independently. This could lead to more nuanced and hierarchical representations of episodic memories, following the underlying semantic structure of the input more closely. Additionally, exploring how EM-LLM could be utilised to enable imagination and future thinking has great potential for advancing model-based reinforcement learning and continual learning techniques in LLMs. By leveraging its event-based structure to simulate potential future scenarios or recall past experiences in novel contexts, EM-LLM could enhance an LLM's ability to plan, adapt, and learn continuously from new information.

6 CONCLUSION

In this work, we introduced EM-LLM, a flexible architecture that integrates key aspects of human episodic memory and event cognition into Transformer-based LLMs. Our approach enables existing

LLMs to effectively process vastly extended contexts without the need for pre-training, demonstrating superior performance on long-context tasks compared to the corresponding SOTA. By combining surprise-based event segmentation, graph-theoretic boundary refinement, and a two-stage memory retrieval process, EM-LLM offers a promising path toward virtually infinite context windows. This capability has the potential to revolutionize interactions with LLMs, enabling continuous, personalised exchanges over extended periods and serving as a viable alternative to traditional RAG techniques. Finally, by bridging insights from cognitive science with machine learning, our approach not only enhances the performance of LLMs on long-context tasks but also provides a scalable framework for computational modelling of episodic and event cognition. We hope this study inspires the community to expand research at the intersection of LLMs and human memory.

REFERENCES

Nelson F Liu, Kevin Lin, John Hewitt, Ashwin Paranjape, Michele Bevilacqua, Fabio Petroni, and Percy Liang. Lost in the middle: How language models use long contexts. *Transactions of the Association for Computational Linguistics*, 12:157–173, 2024a.

Amirhossein Kazemnejad, Inkit Padhi, Karthikeyan Natesan Ramamurthy, Payel Das, and Siva Reddy. The impact of positional encoding on length generalization in transformers. *Advances in Neural Information Processing Systems*, 36, 2024.

Szymon Tworkowski, Konrad Staniszewski, Mikołaj Pacek, Yuhuai Wu, Henryk Michalewski, and Piotr Miłoś. Focused transformer: Contrastive training for context scaling. In *Thirty-seventh Conference on Neural Information Processing Systems*, 2023. URL `https://openreview.net/forum?id=s1FjXzJ0jy`.

Patrick Lewis, Ethan Perez, Aleksandra Piktus, Fabio Petroni, Vladimir Karpukhin, Naman Goyal, Heinrich Küttler, Mike Lewis, Wen-tau Yih, Tim Rocktäschel, et al. Retrieval-augmented generation for knowledge-intensive nlp tasks. *Advances in Neural Information Processing Systems*, 33: 9459–9474, 2020.

Yunfan Gao, Yun Xiong, Xinyu Gao, Kangxiang Jia, Jinliu Pan, Yuxi Bi, Yi Dai, Jiawei Sun, Qianyu Guo, Meng Wang, and Haofen Wang. Retrieval-augmented generation for large language models: A survey, 2024.

Yuhuai Wu, Markus Norman Rabe, DeLesley Hutchins, and Christian Szegedy. Memorizing transformers. In *International Conference on Learning Representations*, 2022. URL `https://openreview.net/forum?id=TrjbxzRcnf-`.

Amanda Bertsch, Uri Alon, Graham Neubig, and Matthew R. Gormley. Unlimiformer: Long-range transformers with unlimited length input. In *Thirty-seventh Conference on Neural Information Processing Systems*, 2023. URL `https://openreview.net/forum?id=lJWUJWLCJo`.

Chaojun Xiao, Pengle Zhang, Xu Han, Guangxuan Xiao, Yankai Lin, Zhengyan Zhang, Zhiyuan Liu, Song Han, and Maosong Sun. Infllm: Unveiling the intrinsic capacity of llms for understanding extremely long sequences with training-free memory. In *Advances in Neural Information Processing Systems*, 2024a. To appear.

Yiran Ding, Li Lyna Zhang, Chengruidong Zhang, Yuanyuan Xu, Ning Shang, Jiahang Xu, Fan Yang, and Mao Yang. Longrope: Extending llm context window beyond 2 million tokens. *arXiv preprint arXiv:2402.13753*, 2024.

David Clewett, Sarah DuBrow, and Lila Davachi. Transcending time in the brain: How event memories are constructed from experience. *Hippocampus*, 29(3):162–183, 2019.

Jeffrey M Zacks. Event perception and memory. *Annual review of psychology*, 71:165–191, 2020.

Christopher Baldassano, Janice Chen, Asieh Zadbood, Jonathan W Pillow, Uri Hasson, and Kenneth A Norman. Discovering event structure in continuous narrative perception and memory. *Neuron*, 95 (3):709–721, 2017.

Sebastian Michelmann, Uri Hasson, and Kenneth A. Norman. Evidence that event boundaries are access points for memory retrieval. *Psychological Science*, 34(3):326–344, 2023a. doi:10.1177/09567976221128206. URL https://doi.org/10.1177/09567976221128206. PMID: 36595492.

Jeffrey M Zacks, Nicole K Speer, Khena M Swallow, Todd S Braver, and Jeremy R Reynolds. Event perception: a mind-brain perspective. *Psychological bulletin*, 133(2):273, 2007.

Jeffrey M Zacks, Christopher A Kurby, Michelle L Eisenberg, and Nayiri Haroutunian. Prediction error associated with the perceptual segmentation of naturalistic events. *Journal of cognitive neuroscience*, 23(12):4057–4066, 2011.

Warrick Roseboom, Zafeirios Fountas, Kyriacos Nikiforou, David Bhowmik, Murray Shanahan, and Anil K Seth. Activity in perceptual classification networks as a basis for human subjective time perception. *Nature communications*, 10(1):267, 2019.

Alyssa H. Sinclair, Grace M. Manalili, Iva K. Brunec, R. Alison Adcock, and Morgan D. Barense. Prediction errors disrupt hippocampal representations and update episodic memories. *Proceedings of the National Academy of Sciences*, 118(51):e2117625118, 2021. doi:10.1073/pnas.2117625118. URL https://www.pnas.org/doi/abs/10.1073/pnas.2117625118.

Zafeirios Fountas, Anastasia Sylaidi, Kyriacos Nikiforou, Anil K. Seth, Murray Shanahan, and Warrick Roseboom. A Predictive Processing Model of Episodic Memory and Time Perception. *Neural Computation*, 34(7):1501–1544, 06 2022. ISSN 0899-7667. doi:10.1162/neco_a_01514. URL https://doi.org/10.1162/neco_a_01514.

Marc W Howard and Michael J Kahana. A distributed representation of temporal context. *Journal of mathematical psychology*, 46(3):269–299, 2002.

Li Ji-An, Corey Y. Zhou, Marcus K. Benna, and Marcelo G. Mattar. Linking in-context learning in transformers to human episodic memory. In *Advances in Neural Information Processing Systems*, 2024. To appear.

Yushi Bai, Xin Lv, Jiajie Zhang, Hongchang Lyu, Jiankai Tang, Zhidian Huang, Zhengxiao Du, Xiao Liu, Aohan Zeng, Lei Hou, Yuxiao Dong, Jie Tang, and Juanzi Li. Longbench: A bilingual, multitask benchmark for long context understanding. *arXiv preprint arXiv:2308.14508*, 2023.

Xinrong Zhang, Yingfa Chen, Shengding Hu, Zihang Xu, Junhao Chen, Moo Khai Hao, Xu Han, Zhen Leng Thai, Shuo Wang, Zhiyuan Liu, et al. $\infty-$bench: Extending long context evaluation beyond 100k tokens. *arXiv preprint arXiv:2402.13718*, 2024.

Manoj Kumar, Ariel Goldstein, Sebastian Michelmann, Jeffrey M Zacks, Uri Hasson, and Kenneth A Norman. Bayesian surprise predicts human event segmentation in story listening. *Cognitive science*, 47(10):e13343, 2023.

Jack W. Rae, Anna Potapenko, Siddhant M. Jayakumar, Chloe Hillier, and Timothy P. Lillicrap. Compressive transformers for long-range sequence modelling. In *International Conference on Learning Representations*, 2020. URL https://openreview.net/forum?id=SylKikSYDH.

Angelos Katharopoulos, Apoorv Vyas, Nikolaos Pappas, and François Fleuret. Transformers are rnns: Fast autoregressive transformers with linear attention. In *International conference on machine learning*, pages 5156–5165. PMLR, 2020.

Tsendsuren Munkhdalai, Manaal Faruqui, and Siddharth Gopal. Leave no context behind: Efficient infinite context transformers with infini-attention, 2024.

Ashish Vaswani, Noam Shazeer, Niki Parmar, Jakob Uszkoreit, Llion Jones, Aidan N Gomez, Łukasz Kaiser, and Illia Polosukhin. Attention is all you need. *Advances in neural information processing systems*, 30, 2017.

Jianlin Su, Murtadha Ahmed, Yu Lu, Shengfeng Pan, Wen Bo, and Yunfeng Liu. Roformer: Enhanced transformer with rotary position embedding. *Neurocomputing*, 568:127063, 2024. ISSN 0925-2312. doi:https://doi.org/10.1016/j.neucom.2023.127063. URL https://www.sciencedirect.com/science/article/pii/S0925231223011864.

Guanzheng Chen, Xin Li, Zaiqiao Meng, Shangsong Liang, and Lidong Bing. CLEX: Continuous length extrapolation for large language models. In *The Twelfth International Conference on Learning Representations*, 2024a. URL `https://openreview.net/forum?id=wXpSidPpc5`.

Wenhan Xiong, Jingyu Liu, Igor Molybog, Hejia Zhang, Prajjwal Bhargava, Rui Hou, Louis Martin, Rashi Rungta, Karthik Abinav Sankararaman, Barlas Oguz, et al. Effective long-context scaling of foundation models. *arXiv preprint arXiv:2309.16039*, 2023.

Xiaoran Liu, Hang Yan, Chenxin An, Xipeng Qiu, and Dahua Lin. Scaling laws of roPE-based extrapolation. In *The Twelfth International Conference on Learning Representations*, 2024b. URL `https://openreview.net/forum?id=JO7k0SJ5V6`.

Bowen Peng, Jeffrey Quesnelle, Honglu Fan, and Enrico Shippole. YaRN: Efficient context window extension of large language models. In *The Twelfth International Conference on Learning Representations*, 2024. URL `https://openreview.net/forum?id=wHBfxhZu1u`.

Ofir Press, Noah A Smith, and Mike Lewis. Train short, test long: Attention with linear biases enables input length extrapolation. *arXiv preprint arXiv:2108.12409*, 2021.

Shouyuan Chen, Sherman Wong, Liangjian Chen, and Yuandong Tian. Extending context window of large language models via positional interpolation. *arXiv preprint arXiv:2306.15595*, 2023.

Hongye Jin, Xiaotian Han, Jingfeng Yang, Zhimeng Jiang, Zirui Liu, Chia-Yuan Chang, Huiyuan Chen, and Xia Hu. Llm maybe longlm: Self-extend llm context window without tuning, 2024.

Ta-Chung Chi, Ting-Han Fan, Peter Ramadge, and Alexander Rudnicky. KERPLE: Kernelized relative positional embedding for length extrapolation. In Alice H. Oh, Alekh Agarwal, Danielle Belgrave, and Kyunghyun Cho, editors, *Advances in Neural Information Processing Systems*, 2022. URL `https://openreview.net/forum?id=hXzOqPlXDwm`.

Shanda Li, Chong You, Guru Guruganesh, Joshua Ainslie, Santiago Ontanon, Manzil Zaheer, Sumit Sanghai, Yiming Yang, Sanjiv Kumar, and Srinadh Bhojanapalli. Functional interpolation for relative positions improves long context transformers. In *The Twelfth International Conference on Learning Representations*, 2024a. URL `https://openreview.net/forum?id=rR03qFesqk`.

Colin Raffel, Noam Shazeer, Adam Roberts, Katherine Lee, Sharan Narang, Michael Matena, Yanqi Zhou, Wei Li, and Peter J. Liu. Exploring the limits of transfer learning with a unified text-to-text transformer. *Journal of Machine Learning Research*, 21(140):1–67, 2020. URL `http://jmlr.org/papers/v21/20-074.html`.

Tri Dao. Flashattention-2: Faster attention with better parallelism and work partitioning. In *The Twelfth International Conference on Learning Representations*, 2024. URL `https://openreview.net/forum?id=mZn2Xyh9Ec`.

Insu Han, Rajesh Jayaram, Amin Karbasi, Vahab Mirrokni, David Woodruff, and Amir Zandieh. Hyperattention: Long-context attention in near-linear time. In *The Twelfth International Conference on Learning Representations*, 2024a. URL `https://openreview.net/forum?id=Eh0Od2BJIM`.

Reza Yazdani Aminabadi, Samyam Rajbhandari, Ammar Ahmad Awan, Cheng Li, Du Li, Elton Zheng, Olatunji Ruwase, Shaden Smith, Minjia Zhang, Jeff Rasley, and Yuxiong He. Deepspeed-inference: enabling efficient inference of transformer models at unprecedented scale. In *Proceedings of the International Conference on High Performance Computing, Networking, Storage and Analysis*, SC '22. IEEE Press, 2022. ISBN 9784665454445.

Woosuk Kwon, Zhuohan Li, Siyuan Zhuang, Ying Sheng, Lianmin Zheng, Cody Hao Yu, Joseph Gonzalez, Hao Zhang, and Ion Stoica. Efficient memory management for large language model serving with pagedattention. In *Proceedings of the 29th Symposium on Operating Systems Principles*, SOSP '23, page 611–626, New York, NY, USA, 2023. Association for Computing Machinery. ISBN 9798400702297. doi:10.1145/3600006.3613165. URL `https://doi.org/10.1145/3600006.3613165`.

Hao Liu, Matei Zaharia, and Pieter Abbeel. Ringattention with blockwise transformers for near-infinite context. In *The Twelfth International Conference on Learning Representations*, 2024c. URL https://openreview.net/forum?id=WsRHpHH4s0.

William Brandon, Aniruddha Nrusimha, Kevin Qian, Zachary Ankner, Tian Jin, Zhiye Song, and Jonathan Ragan-Kelley. Striped attention: Faster ring attention for causal transformers. *arXiv preprint arXiv:2311.09431*, 2023.

Piotr Nawrot, Adrian Łańcucki, Marcin Chochowski, David Tarjan, and Edoardo M Ponti. Dynamic memory compression: Retrofitting llms for accelerated inference. *arXiv preprint arXiv:2403.09636*, 2024.

Zhenyu Zhang, Ying Sheng, Tianyi Zhou, Tianlong Chen, Lianmin Zheng, Ruisi Cai, Zhao Song, Yuandong Tian, Christopher Re, Clark Barrett, Zhangyang Wang, and Beidi Chen. H2o: Heavy-hitter oracle for efficient generative inference of large language models. In *Thirty-seventh Conference on Neural Information Processing Systems*, 2023. URL https://openreview.net/forum?id=RkRrPp7GKO.

Dawei Zhu, Nan Yang, Liang Wang, Yifan Song, Wenhao Wu, Furu Wei, and Sujian Li. PoSE: Efficient context window extension of LLMs via positional skip-wise training. In *The Twelfth International Conference on Learning Representations*, 2024. URL https://openreview.net/forum?id=3Z1gxuAQrA.

Yukang Chen, Shengju Qian, Haotian Tang, Xin Lai, Zhijian Liu, Song Han, and Jiaya Jia. LongloRA: Efficient fine-tuning of long-context large language models. In *The Twelfth International Conference on Learning Representations*, 2024b. URL https://openreview.net/forum?id=6PmJoRfdaK.

Weizhi Wang, Li Dong, Hao Cheng, Xiaodong Liu, Xifeng Yan, Jianfeng Gao, and Furu Wei. Augmenting language models with long-term memory. In *Thirty-seventh Conference on Neural Information Processing Systems*, 2023. URL https://openreview.net/forum?id=BryMFPQ4L6.

Maor Ivgi, Uri Shaham, and Jonathan Berant. Efficient long-text understanding with short-text models. *Transactions of the Association for Computational Linguistics*, 11:284–299, 2023. doi:10.1162/tacl_a_00547. URL https://aclanthology.org/2023.tacl-1.17.

Samuel J Gershman, Christopher D Moore, Michael T Todd, Kenneth A Norman, and Per B Sederberg. The successor representation and temporal context. *Neural Computation*, 24(6):1553–1568, 2012.

Marcus K Benna and Stefano Fusi. Place cells may simply be memory cells: Memory compression leads to spatial tuning and history dependence. *Proceedings of the National Academy of Sciences*, 118(51):e2018422118, 2021.

Charles Blundell, Benigno Uria, Alexander Pritzel, Yazhe Li, Avraham Ruderman, Joel Z Leibo, Jack Rae, Daan Wierstra, and Demis Hassabis. Model-free episodic control. *arXiv preprint arXiv:1606.04460*, 2016.

Alexander Pritzel, Benigno Uria, Sriram Srinivasan, Adrià Puigdomènech Badia, Oriol Vinyals, Demis Hassabis, Daan Wierstra, and Charles Blundell. Neural episodic control. In Doina Precup and Yee Whye Teh, editors, *Proceedings of the 34th International Conference on Machine Learning*, volume 70 of *Proceedings of Machine Learning Research*, pages 2827–2836. PMLR, 06–11 Aug 2017.

Julian Coda-Forno, Changmin Yu, Qinghai Guo, Zafeirios Fountas, and Neil Burgess. Leveraging episodic memory to improve world models for reinforcement learning. In *Memory in Artificial and Real Intelligence (MemARI) Workshop at 36th Conference on Neural Information Processing Systems (NeurIPS 2022)*, 2024.

James Kirkpatrick, Razvan Pascanu, Neil Rabinowitz, Joel Veness, Guillaume Desjardins, Andrei A Rusu, Kieran Milan, John Quan, Tiago Ramalho, Agnieszka Grabska-Barwinska, et al. Overcoming catastrophic forgetting in neural networks. *Proceedings of the national academy of sciences*, 114 (13):3521–3526, 2017.

David Lopez-Paz and Marc' Aurelio Ranzato. Gradient episodic memory for continual learning. In I. Guyon, U. Von Luxburg, S. Bengio, H. Wallach, R. Fergus, S. Vishwanathan, and R. Garnett, editors, *Advances in Neural Information Processing Systems*, volume 30. Curran Associates, Inc., 2017. URL `https://proceedings.neurips.cc/paper_files/paper/2017/file/f87522788a2be2d171666752f97ddebb-Paper.pdf`.

Arslan Chaudhry, Marc'Aurelio Ranzato, Marcus Rohrbach, and Mohamed Elhoseiny. Efficient lifelong learning with a-GEM. In *International Conference on Learning Representations*, 2019. URL `https://openreview.net/forum?id=Hkf2_sC5FX`.

Pietro Buzzega, Matteo Boschini, Angelo Porrello, Davide Abati, and SIMONE CALDERARA. Dark experience for general continual learning: a strong, simple baseline. In H. Larochelle, M. Ranzato, R. Hadsell, M.F. Balcan, and H. Lin, editors, *Advances in Neural Information Processing Systems*, volume 33, pages 15920–15930. Curran Associates, Inc., 2020. URL `https://proceedings.neurips.cc/paper_files/paper/2020/file/b704ea2c39778f07c617f6b7ce480e9e-Paper.pdf`.

Ameya Prabhu, Philip H. S. Torr, and Puneet K. Dokania. Gdumb: A simple approach that questions our progress in continual learning. In Andrea Vedaldi, Horst Bischof, Thomas Brox, and Jan-Michael Frahm, editors, *Computer Vision – ECCV 2020*, pages 524–540, Cham, 2020. Springer International Publishing.

Payel Das, Subhajit Chaudhury, Elliot Nelson, Igor Melnyk, Sarath Swaminathan, Sihui Dai, Aurélie Lozano, Georgios Kollias, Vijil Chenthamarakshan, Soham Dan, et al. Larimar: Large language models with episodic memory control. *arXiv preprint arXiv:2403.11901*, 2024.

Eleanor Spens and Neil Burgess. A generative model of memory construction and consolidation. *Nature Human Behaviour*, pages 1–18, 2024.

Qihong Lu, Uri Hasson, and Kenneth A Norman. A neural network model of when to retrieve and encode episodic memories. *elife*, 11:e74445, 2022.

Maxine T Sherman, Zafeirios Fountas, Anil K Seth, and Warrick Roseboom. Trial-by-trial predictions of subjective time from human brain activity. *PLOS Computational Biology*, 18(7):e1010223, 2022.

Alexey Zakharov, Qinghai Guo, and Zafeirios Fountas. Variational predictive routing with nested subjective timescales. In *International Conference on Learning Representations*, 2022a. URL `https://openreview.net/forum?id=JxFgJbZ-wft`.

Alexey Zakharov, Qinghai Guo, and Zafeirios Fountas. Long-horizon video prediction using a dynamic latent hierarchy. *arXiv preprint arXiv:2212.14376*, 2022b.

Alexey Zakharov, Matthew Crosby, and Zafeirios Fountas. Episodic memory for subjective-timescale models. In *ICML 2021 Workshop on Unsupervised Reinforcement Learning*, 2021. URL `https://openreview.net/forum?id=30lZDhrjonR`.

Nelson Cowan. The magical number 4 in short-term memory: A reconsideration of mental storage capacity. *Behavioral and brain sciences*, 24(1):87–114, 2001.

Guangxuan Xiao, Yuandong Tian, Beidi Chen, Song Han, and Mike Lewis. Efficient streaming language models with attention sinks. In *The Twelfth International Conference on Learning Representations*, 2024b. URL `https://openreview.net/forum?id=NG7sS51zVF`.

Chi Han, Qifan Wang, Hao Peng, Wenhan Xiong, Yu Chen, Heng Ji, and Sinong Wang. LM-infinite: Zero-shot extreme length generalization for large language models. In Kevin Duh, Helena Gomez, and Steven Bethard, editors, *Proceedings of the 2024 Conference of the North American Chapter of the Association for Computational Linguistics: Human Language Technologies (Volume 1: Long Papers)*, pages 3991–4008, Mexico City, Mexico, June 2024b. Association for Computational Linguistics. URL `https://aclanthology.org/2024.naacl-long.222`.

Pierre Miasnikof, Alexander Shestopaloff, Anthony Bonner, and Yuri Lawryshyn. *A Statistical Performance Analysis of Graph Clustering Algorithms*, pages 170–184. 05 2018. ISBN 978-3-319-92870-8. doi:10.1007/978-3-319-92871-5_11.

Mark EJ Newman and Michelle Girvan. Finding and evaluating community structure in networks. *Physical review E*, 69(2):026113, 2004.

Matthijs Douze, Alexandr Guzhva, Chengqi Deng, Jeff Johnson, Gergely Szilvasy, Pierre-Emmanuel Mazaré, Maria Lomeli, Lucas Hosseini, and Hervé Jégou. The faiss library. 2024.

Chankyu Lee, Rajarshi Roy, Mengyao Xu, Jonathan Raiman, Mohammad Shoeybi, Bryan Catanzaro, and Wei Ping. Nv-embed: Improved techniques for training llms as generalist embedding models. *arXiv preprint arXiv:2405.17428*, 2024.

Zhuowan Li, Cheng Li, Mingyang Zhang, Qiaozhu Mei, and Michael Bendersky. Retrieval augmented generation or long-context llms? a comprehensive study and hybrid approach, 2024b. URL https://arxiv.org/abs/2407.16833.

Sebastian Michelmann, Amy R Price, Bobbi Aubrey, Camilla K Strauss, Werner K Doyle, Daniel Friedman, Patricia C Dugan, Orrin Devinsky, Sasha Devore, Adeen Flinker, et al. Moment-by-moment tracking of naturalistic learning and its underlying hippocampo-cortical interactions. *Nature communications*, 12(1):5394, 2021.

Olga Lositsky, Janice Chen, Daniel Toker, Christopher J Honey, Michael Shvartsman, Jordan L Poppenk, Uri Hasson, and Kenneth A Norman. Neural pattern change during encoding of a narrative predicts retrospective duration estimates. *elife*, 5:e16070, 2016.

Alberto Mariola, Zafeirios Fountas, Lionel Barnett, and Warrick Roseboom. Event segmentation in continuous, naturalistic videos from model-based, data-driven, and human perspectives. 2022.

Sebastian Michelmann, Manoj Kumar, Kenneth A Norman, and Mariya Toneva. Large language models can segment narrative events similarly to humans. *arXiv preprint arXiv:2301.10297*, 2023b.

Alan Baddeley. Working memory: looking back and looking forward. *Nature reviews neuroscience*, 4(10):829–839, 2003.

K Anders Ericsson and Walter Kintsch. Long-term working memory. *Psychological review*, 102(2): 211, 1995.

Santo Fortunato. Community detection in graphs. *Physics reports*, 486(3-5):75–174, 2010.

Zhao Yang, René Algesheimer, and Claudio J Tessone. A comparative analysis of community detection algorithms on artificial networks. *Scientific reports*, 6(1):30750, 2016.

Ryan Prescott Adams and David JC MacKay. Bayesian online changepoint detection. *arXiv preprint arXiv:0710.3742*, 2007.

Zhuowan Li, Cheng Li, Mingyang Zhang, Qiaozhu Mei, and Michael Bendersky. Retrieval augmented generation or long-context llms? a comprehensive study and hybrid approach. *arXiv preprint arXiv:2407.16833*, 2024c.

Nils Reimers. Sentence-transformers: all-mpnet-base-v2. Hugging Face Model Hub, 2022. Available from: https://huggingface.co/sentence-transformers/all-mpnet-base-v2.

Niklas Muennighoff, Nouamane Tazi, Loïc Magne, and Nils Reimers. Mteb: Massive text embedding benchmark. *arXiv preprint arXiv:2210.07316*, 2022.

Rolf Jagerman, Honglei Zhuang, Zhen Qin, Xuanhui Wang, and Michael Bendersky. Query expansion by prompting large language models, 2023. URL https://arxiv.org/abs/2305.03653.

Yunxiao Shi, Xing Zi, Zijing Shi, Haimin Zhang, Qiang Wu, and Min Xu. Eragent: Enhancing retrieval-augmented language models with improved accuracy, efficiency, and personalization, 2024. URL https://arxiv.org/abs/2405.06683.

Sagnik Majumder, Chinmoy Samant, and Greg Durrett. Model agnostic answer reranking system for adversarial question answering. *CoRR*, abs/2102.03016, 2021. URL https://arxiv.org/abs/2102.03016.

Victor M. Panaretos and Yoav Zemel. Statistical aspects of wasserstein distances. *Annual Review of Statistics and Its Application*, 6(Volume 6, 2019):405–431, 2019. ISSN 2326-831X. doi:https://doi.org/10.1146/annurev-statistics-030718-104938. URL https://www.annualreviews.org/content/journals/10.1146/annurev-statistics-030718-104938.

Mark EJ Newman. Fast algorithm for detecting community structure in networks. *Physical Review E—Statistical, Nonlinear, and Soft Matter Physics*, 69(6):066133, 2004.

List of Appendices

A ANALYTICAL RESULTS

A.1 COMPARISON WITH KV-RETRIEVAL-BASED LLMS

Task	InfLLM	Max Imp.	EM-LLM			
			S	SM	S+C	SM+C
NarrativeQA	22.12	**1.49%**	21.77	21.13	21.10	**22.45**
Qasper	29.33	**0.17%**	29.07	**29.38**	29.16	28.68
MultiFieldQA	47.42	**1.46%**	**48.11**	47.39	47.72	47.62
HotpotQA	36.56	**10.15%**	39.40	39.01	**40.27**	38.90
2WikiMQA	22.31	**5.20%**	23.46	22.75	**23.47**	23.46
Musique	17.68	**6.17%**	17.97	17.82	17.98	**18.77**
GovReport	31.03	**1.90%**	31.40	**31.62**	31.10	31.43
QMSum	23.49	**2.13%**	**23.99**	23.20	23.48	23.47
MultiNews	**26.70**	-0.30%	26.55	26.54	26.58	26.62
TREC	69.00	**2.90%**	**71.00**	70.00	70.50	70.50
TriviaQA	86.67	**1.10%**	86.58	**87.62**	87.52	87.47
SAMSum	42.52	**0.45%**	**42.71**	42.13	42.34	42.48
PassageRetrieval	64.00	**32.69%**	82.67	78.92	**84.92**	84.08
LCC	56.67	**0.64%**	55.03	**57.03**	54.90	56.79
RepoBench-P	52.97	**1.34%**	50.49	**53.68**	51.06	52.86
Avg. score:	41.90	**4.50%**	43.35	43.22	43.47	**43.71**
Code.Debug	29.44	**0.88%**	**29.70**	28.43	28.68	28.17
Math.Find	26.57	**5.38%**	**28.00**	27.43	27.71	27.14
Retrieve.KV	95.60	**3.56%**	92.20	97.20	97.60	**99.00**
En.MC	**43.23**	-1.02%	41.48	40.61	42.79	42.79
Retrieve.PassKey	**100.00**	0.00%	**100.00**	**100.00**	**100.00**	**100.00**
Retrieve.Number	**99.83**	0.00%	**99.83**	**99.83**	**99.83**	**99.83**
Avg. score:	65.78	**1.47%**	65.20	65.58	66.10	**66.16**

Table 3: EM-LLM performance on LongBench and ∞-Bench (respectively) compared to our baseline, InfLLM, with Mistral-7B-Instruct-v0.2 as the base LLM and 4K+2K context. **S**: surprise threshold, **SM**: surprise threshold + refinement with modularity, **S+C**: surprise threshold + contiguity buffer, **SM+C**: surprise threshold + refinement with modularity + contiguity buffer. **Max Imp.**: Maximum relative improvement over InfLLM across all EM-LLM variants.

Task	InfLLM	Max Imp.	EM-LLM			
			S	SM	S+C	SM+C
NarrativeQA	22.64	**8.92%**	24.47	22.50	**24.66**	23.03
Qasper	43.70	**3.25%**	44.35	44.95	45.07	**45.12**
MultiFieldQA	49.03	**0.47%**	49.11	48.79	**49.26**	48.36
HotpotQA	49.04	**0.69%**	48.97	49.19	48.74	**49.38**
2WikiMQA	35.61	**8.26%**	38.44	38.08	**38.55**	38.08
Musique	**26.06**	-1.46%	25.68	25.19	24.64	23.92
GovReport	30.76	**1.11%**	**31.10**	30.85	30.96	30.86
QMSum	22.70	**0.31%**	22.63	**22.77**	22.62	22.58
MultiNews	**27.57**	-0.91%	27.32	27.28	27.30	27.29
TREC	73.50	0.00%	73.50	73.50	73.50	73.50
TriviaQA	90.91	0.00%	90.91	90.91	90.91	90.91
SAMSum	42.43	**1.98%**	43.24	**43.27**	42.91	42.84
PassageRetrieval	84.00	**4.17%**	**87.50**	86.00	86.00	85.00
LCC	59.88	**0.94%**	58.49	**60.44**	58.55	60.41
RepoBench-P	**46.48**	-3.44%	42.13	44.88	42.26	44.68
Avg. score:	46.95	**1.62%**	47.19	**47.24**	47.06	47.06
Code.Debug	30.46	**5.81%**	31.73	30.20	**32.23**	31.73
Math.Find	**23.70**	-27.68%	16.86	16.57	16.29	17.14
Retrieve.KV	5.00	**4.00%**	4.20	4.80	**5.20**	5.00
En.MC	**43.70**	-3.07%	40.55	42.36	39.74	40.61
Retrieve.PassKey	**100.00**	0.00%	**100.00**	**100.00**	**100.00**	**100.00**
Retrieve.Number	99.00	**0.67%**	99.49	99.49	**99.66**	99.49
Avg. score:	**50.31**	-3.38%	48.81	48.90	48.85	49.00

Table 4: EM-LLM performance on LongBench and ∞-Bench (respectively) compared to our baseline, InfLLM, with LLaMA-3-8B-Instruct as the base LLM and 4K+4K context. Abbreviations as before.

Task	InfLLM	Max Imp.	EM-LLM			
			S	SM	S+C	SM+C
NarrativeQA	26.64	**2.25%**	26.05	26.05	**27.24**	25.98
Qasper	44.95	**1.27%**	44.41	**45.52**	44.71	45.41
MultiFieldQA	**52.56**	-0.08%	52.52	52.07	52.36	52.48
HotpotQA	52.96	**2.00%**	**54.02**	52.49	53.37	53.90
2WikiMQA	45.04	**4.57%**	45.72	45.60	46.61	**47.10**
Musique	23.98	**7.76%**	25.37	**25.84**	24.60	24.73
GovReport	34.96	**0.57%**	35.04	**35.16**	34.94	34.81
QMSum	24.36	**0.94%**	24.31	24.55	24.31	**24.59**
MultiNews	27.78	**0.14%**	27.76	27.79	**27.82**	27.77
TREC	71.00	**0.70%**	71.50	71.50	71.50	71.00
TriviaQA	**92.44**	0.00%	92.34	92.24	92.43	**92.44**
SAMSum	43.68	**0.41%**	43.31	43.65	43.63	**43.86**
PassageRetrieval	97.00	**2.58%**	**99.50**	98.50	98.00	97.50
LCC	65.82	**2.48%**	**67.45**	65.69	65.74	65.74
RepoBench-P	62.56	**2.83%**	**64.33**	62.54	62.18	61.87
Avg. score:	51.05	**1.89%**	**51.58**	51.28	51.30	51.28
Code.Debug	**22.59**	0.00%	**22.59**	**22.59**	**22.59**	**22.59**
Math.Find	33.71	**6.79%**	**36.00**	34.00	35.43	27.71
Retrieve.KV	81.00	**19.51%**	**96.80**	90.20	95.40	95.20
En.MC	46.72	**1.88%**	44.54	**47.60**	46.72	45.85
Retrieve.PassKey	**100.00**	0.00%	**100.00**	**100.00**	**100.00**	**100.00**
Retrieve.Number	**100.00**	0.00%	**100.00**	**100.00**	**100.00**	**100.00**
Avg. score:	64.00	**4.70%**	66.66	65.73	**66.69**	65.23

Table 5: EM-LLM performance on LongBench and ∞-Bench (respectively) compared to our baseline, InfLLM, with LLaMA-3.1-8B-Instruct as the base LLM and 4K+4K context. Abbreviations as before.

Task	InfLLM	Max Imp.	EM-LLM			
			S	SM	S+C	SM+C
NarrativeQA	14.82	**14.04%**	15.78	**16.90**	16.02	16.66
Qasper	28.71	**5.29%**	28.25	28.46	29.10	**30.23**
MultiFieldQA	41.54	**5.66%**	43.48	**43.89**	42.57	42.57
HotpotQA	32.64	**10.45%**	**36.05**	34.37	33.53	31.98
2WikiMQA	27.08	**10.16%**	28.74	28.05	**29.83**	27.49
Musique	15.05	**29.70%**	16.53	16.76	**19.52**	16.49
GovReport	28.96	**2.97%**	29.41	29.59	**29.82**	29.62
QMSum	21.64	**3.00%**	**22.29**	21.90	22.06	22.07
MultiNews	**26.32**	-0.49%	26.07	26.16	25.89	26.19
TREC	67.00	**3.73%**	68.50	**69.50**	68.50	68.00
TriviaQA	83.71	**1.73%**	83.59	84.16	**85.16**	85.09
SAMSum	7.83	**8.30%**	8.43	**8.48**	7.28	8.06
PassageRetrieval	7.50	**40.00%**	10.00	9.50	9.00	**10.50**
LCC	**60.33**	-0.22%	59.99	60.13	60.20	60.01
RepoBench-P	53.70	**0.37%**	**53.90**	53.59	53.44	53.27
Avg. score:	34.46	**8.98%**	35.40	35.43	**35.46**	35.22

Table 6: EM-LLM performance on LongBench compared to our baseline, InfLLM, with Phi-3-Mini-4K-Instruct as the base LLM and 1K+3K context. Abbreviations as before.

Task	InfLLM	Max Imp.	EM-LLM			
			S	SM	S+C	SM+C
NarrativeQA	17.82	**8.98%**	**19.42**	16.63	17.55	17.12
Qasper	31.44	**3.34%**	32.38	31.71	31.43	**32.49**
MultiFieldQA	**45.80**	-2.36%	43.58	44.72	44.28	44.66
HotpotQA	41.33	**11.35%**	**46.02**	44.78	44.43	44.89
2WikiMQA	27.74	**8.51%**	29.68	28.68	**30.10**	29.27
Musique	16.39	**21.23%**	**19.87**	19.26	18.70	19.41
GovReport	26.37	**3.22%**	27.05	**27.22**	26.76	27.13
QMSum	21.19	**4.29%**	21.94	**22.10**	21.79	21.79
MultiNews	24.23	**0.70%**	24.39	24.29	24.29	**24.40**
TREC	67.50	**2.22%**	67.50	**69.00**	67.50	68.00
TriviaQA	**84.66**	-0.99%	83.82	83.82	83.82	83.49
SAMSum	**16.62**	-0.54%	15.30	14.49	16.53	15.25
PassageRetrieval	11.50	**17.39%**	13.00	**13.50**	13.00	**13.50**
LCC	**38.38**	-3.20%	36.79	37.15	36.90	37.02
RepoBench-P	42.30	**1.75%**	42.16	**43.04**	41.91	41.65
Avg. score:	34.22	**5.06%**	**34.86**	34.69	34.60	34.67

Table 7: EM-LLM performance on LongBench compared to our baseline, InfLLM, with Phi-3.5-mini-Instruct as the base LLM and 1K+3K context. Abbreviations as before.

EXPERIMENT DETAILS

In our experiments with Retrieval-Augmented Generation (RAG) baselines, we implemented a standard RAG pipeline consisting of a retriever and a downstream LLM. For each example in a benchmark task, the example context is split into chunks of l words each and encoded using the retriever's embedding model into a vector database. A similarity lookup into the vector database is used to retrieve the top k most relevant chunks, which are then fed to the downstream LLM alongside the query and task description. For all experiments, we set $l = 300$ and $k = 5$, following the protocol of Li et al. (2024c).

We conducted experiments using two retriever models—NV-Embed-v2 (Lee et al., 2024) and all-mpnet-base-v2 (Reimers, 2022). NV-Embed-v2 is a SOTA LLM-based retriever that uses that, as of September 2024, ranks first on the Massive Text Embedding Benchmark (MTEB) Leaderboard (Muennighoff et al., 2022). It is a fine-tuned Mistral-7Bv0.1 model with an embedding dimension of 4096, trained using contrastive instruction-tuning on both retrieval and non-retrieval datasets. all-mpnet-base-v2 is a smaller 110M parameter model with an embedding size of 768, built on the BERT-base-uncased architecture, trained using contrastive learning on a dataset of over 1 billion sentence pairs. For each embedding model, we ran experiments using LLaMa-3-8B and LLaMa-3.1-8B as the downstream LLM.

LIMITATIONS OF RAG

RAG requires the use of additional modules alongside the downstream LLM during the generation process, meaning that the quality of the generated output depends on the representational capacity of these modules in addition to the capability of the LLM. For example, the use of a retriever model that has far fewer parameters than the downstream LLM can limit the LLM's ability to generate the most accurate or contextually appropriate responses, as shown by the gap in performance between the two RAG pipelines on LongBench shown in Table 8. In this case, whilst the downstream LLM may be capable of high performance on a given task, the retriever may not be expressive enough to provide the relevant context needed to solve said task. Additional pre/post-retrieval techniques such as query expansion (Jagerman et al. (2023)), knowledge filtering (Shi et al. (2024)) or answer reranking (Majumder et al. (2021)), may help to bridge potential performance bottlenecks, but these involve further increasing the complexity of the generation pipeline. In contrast, EM-LLM outperforms both RAG models whilst only requiring the use of a single LLM across the entire generation stage, removing the issue of performance bottlenecks seen in RAG pipelines. Furthermore, EM-LLM is a general purpose method that can be applied to practically any existing transformer LLM - our method was implemented using a general purpose patch to attention layer modules that provided compatibility with the Huggingface Transformers Library.

Task	RAG		EM-LLM$_{SM}$
	all-mpnet-base-v2	NV-Embed-v2	
NarrativeQA	17.31	21.39	**22.50**
Qasper	40.66	41.01	**44.95**
MultiFieldQA	45.16	**50.47**	48.79
HotpotQA	43.32	**53.64**	49.19
2WikiMQA	**41.48**	40.41	38.08
Musique	26.78	**31.56**	25.19
GovReport	27.87	29.26	**30.85**
QMSum	22.44	**23.15**	22.77
MultiNews	26.04	**27.48**	27.28
TREC	4.50	65.00	**73.50**
TriviaQA	78.98	63.75	**90.91**
SAMSum	9.00	32.85	**43.27**
PassageRetrieval	54.00	54.50	**86.00**
LCC	10.76	19.88	**60.44**
RepoBench-P	13.02	34.77	**44.88**
Avg. score:	30.75	39.27	**47.24**

Table 8: Comparison of RAG with two different retrievers vs. EM-LLM on the LongBench dataset. All methods use LLaMa-3-8B-Instruct for generation.

Task	RAG	FC	EM-LLM
NarrativeQA	22.54	**29.14**	26.05
Qasper	**45.45**	45.34	44.41
MultiFieldQA	51.67	**54.98**	52.52
HotpotQA	**55.93**	54.01	54.02
2WikiMQA	42.93	**45.95**	45.72
Musique	30.90	**33.52**	25.37
GovReport	29.91	34.49	**35.04**
QMSum	**24.97**	25.14	24.31
MultiNews	26.77	27.00	**27.76**
TREC	22.50	4.50	**71.50**
TriviaQA	88.11	89.07	**92.34**
SAMSum	7.56	8.68	**43.31**
PassageRetrieval	65.50	**100.00**	99.50
LCC	13.16	19.30	**67.45**
RepoBench-P	18.66	18.33	**64.33**
Avg. score:	36.44	39.30	**51.58**
Code.Debug	**22.59**	21.70	22.59
Math.Find	35.43	26.29	**36.00**
Retrieve.KV	31.80	92.60	**96.80**
En.MC	**64.19**	58.07	44.54
Retrieve.PassKey	**100.00**	**100.00**	**100.00**
Retrieve.Number	99.83	99.32	**100.00**
Avg. score:	58.97	66.33	**66.66**

Table 9: EM-LLM$_S$ (4K+4K) vs. RAG (NV-Embed-v2 retriever) vs. full-context, with LLaMa-3.1-8B as the base LLM, evaluated on LongBench and ∞-Bench.
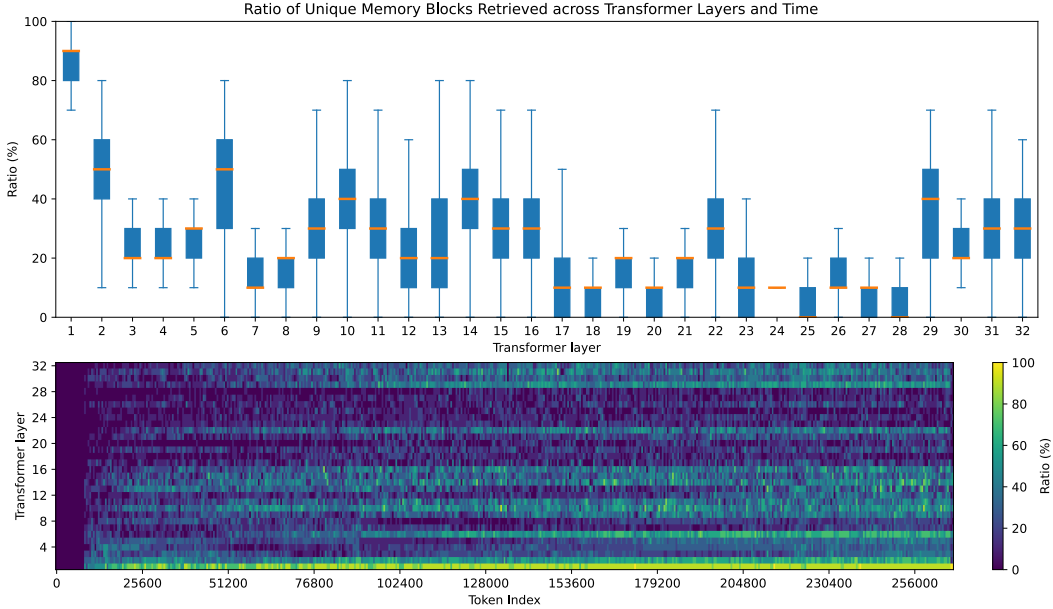

Figure 5: The ratio of blocks retrieved by a layer which were not retrieved by any other layer for the same processed chunk, versus the total number of retrieved blocks by that layer. This is measured using EM-LLM$_S$ with Mistral-7B on a single example of ∞-Bench's *Longbook.Choice.Eng* task, with over 500 chunks of 512 tokens. In RAG methods, this ratio would always be zero, as retrieved blocks are used by all layers concurrently.

B HUMAN DATA

B.1 ANALYSIS

The human data released as part of Kumar et al. (2023) used Gaussian smoothing on the average signal across participants to define a probability distribution of likely event boundary positions with respect to timestamps in the podcast. In order to calculate our similarity metrics, as shown in Fig. 4A, we need to express this data in terms of discrete event positions with respect to tokens in the transcript. For fair comparison, we therefore identified human-annotated positions by selecting as many of the most likely positions in the distribution as our initial surprise-based event segmentation had identified in the transcript. In the same process used by Kumar et al. (2023), we then used their provided word onset times to translate these timestamps to token positions, allowing us to calculate our similarity metrics.

In Fig. 4B, we use Wasserstein distance in order to compare the relative positions of event boundaries between human annotations and those found by our own methods. Wasserstein distance is a versatile metric used to compare two probability distributions (Panaretos and Zemel, 2019). We used such a metric to better capture the uncertainty present in the human data, and found it to give more meaningful results than standard correlation or discrete distance metrics, which showed very little differences between methods. In order to calculate such a metric, we therefore need to convert our own discrete boundary positions to a distribution across token positions. We did so by defining a Mixture of Gaussians (MoG), with each Gaussian corresponding to a single position. Note that, for fair comparison with human data, we apply the same process to the discrete version of the human-annotated positions described above, and use this for comparison.
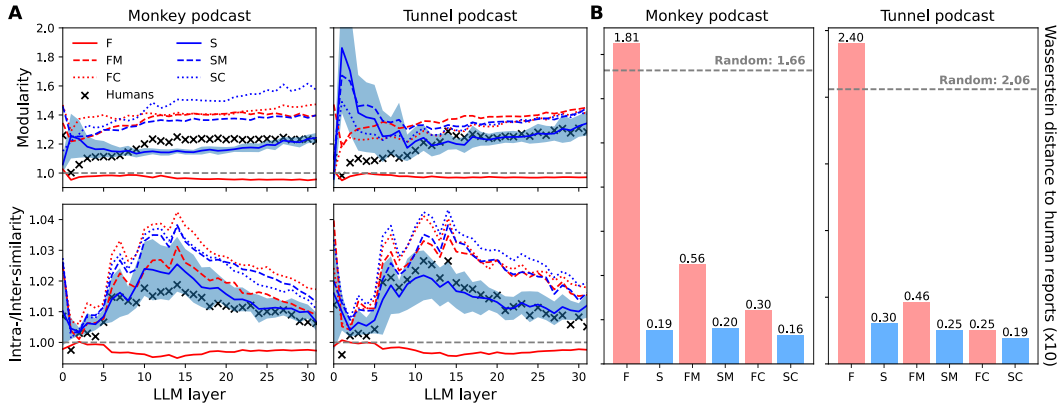
B.2 FURTHER RESULTS

Figure 6: Comparison of human event segmentation with different computational segmentation methods in two human-annotated audio datasets. **(A)** Difference in metrics for the cohesion and separation of KV cache of LLaMA2 attention heads. The graphs report the difference of each method with the corresponding random segmentation. **(B)** Distance between human reports and different methods. In both sets of results, fixed methods (*F*, *FM*, *FC*) perform worse than their surprise-based counterparts (*S*, *SM*, *SC*) with InfLLM's method (*F*) performing worse than random.
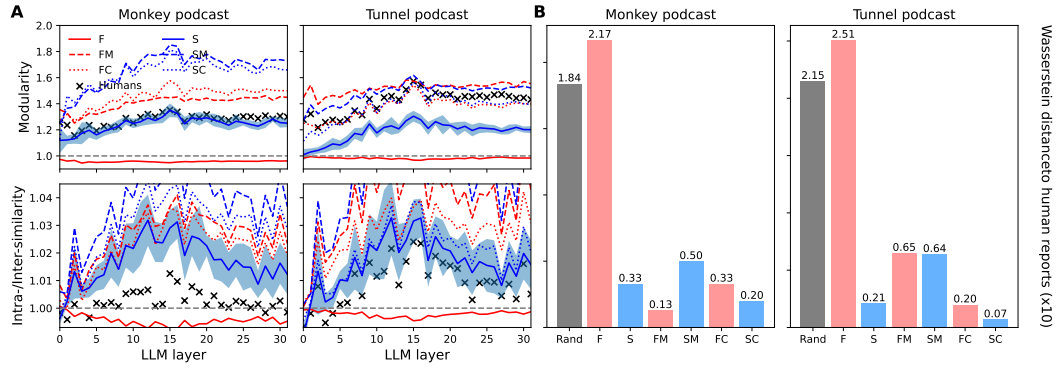
Figure 7: Comparison of human event segmentation with different computational segmentation methods using Mistral-7B. Plots include abbreviations like before.
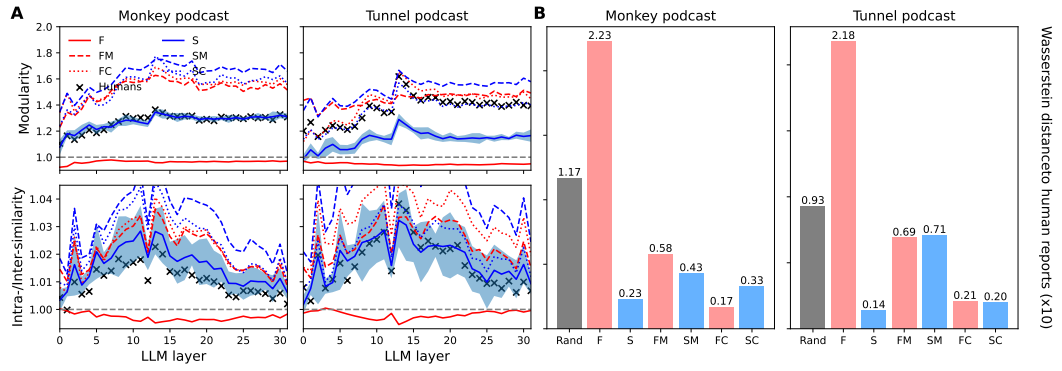

Figure 8: Comparison of human event segmentation with different computational segmentation methods using LLaMA-3-8B-Instruct. Plots include abbreviations like before.

C COMPLEXITY

C.1 COMPLEXITY ANALYSIS

Here, we provide a detailed analysis of the computational complexity of our Algorithm 1, focusing on the boundary refinement step and the calculation of modularity and conductance metrics.

Boundary Refinement Step The boundary refinement step involves finding the optimal position $\hat{\beta}$ between each pair of consecutive initial boundaries (α, β) that optimizes the chosen metric function f. This step has the following components:

Iteration over initial boundaries: $\mathcal{O}(k)$, where k is the number of initial boundaries. For each pair of boundaries, we compute the metric function f for all positions between α and β. In the worst case, this is $\mathcal{O}(n)$ operations per boundary pair.

Therefore, the overall complexity of this step is $\mathcal{O}(kn)$.

Metric Function Computation The metric functions (modularity or conductance) are computed at the level of individual memory units. For a memory unit of size m:

- *Modularity*: The naive computation involves summing over all pairs of nodes within the unit, resulting in a worst-case complexity of $\mathcal{O}(m^2)$. However, in practice, the similarity graph is often sparse, meaning many node pairs have negligible similarity. Leveraging this sparsity, more efficient implementations can achieve $\mathcal{O}(l)$ complexity, where l is the number of non-zero similarity edges within the unit (Newman, 2004). Typically, l is much smaller than m^2, especially for larger units, leading to significant computational savings.
- *Conductance*: This requires computing the sum of edge weights crossing the boundary and the total volume of the unit, which can be done in $\mathcal{O}(m)$ time.

Given that m is typically much smaller than n and varies for each unit, we can consider the average unit size $\bar{m}$ and average number of non-zero similarity edges $\bar{l}$. The total complexity for computing metrics across all units is then $\mathcal{O}(k\bar{l})$ for modularity (which in the worst case is $\mathcal{O}(k\bar{m}^2)$, but typically much lower) or $\mathcal{O}(k\bar{m})$ for conductance.

Overall Complexity Combining the boundary refinement step and metric computation, the overall complexity is:

For modularity: $\mathcal{O}(kn + k\bar{m}^2)$ For conductance: $\mathcal{O}(kn + k\bar{m})$

Since typically $\bar{m} \ll n$, the dominant term in both cases is $\mathcal{O}(kn)$. Therefore, we express the overall complexity of our algorithm as $\mathcal{O}(kn)$.

C.2 IMPLEMENTATION AND USE OF HARDWARE RESOURCES

Retrieval-based methods for handling long sequence lengths can be especially appealing to those who may not have access to the hardware resources necessary to run large, long-context models. In this spirit, we describe here our adjustments to our framework made to further lower the minimum hardware requirements to accurately run inference on sequence lengths of 1M+ tokens. We note that our approach is very scalable in the sense that handling longer contexts only requires an increase in CPU memory, or even just disk storage.

All of our experiments were run on single nodes of 4 GPUs, each with 32GB of dedicated memory (except for the full-context results for which we used an API). Additionally, each node had a minimum of 100GB of CPU memory. While all base models and methods used across our own experiments fit on a single GPU, such hardware is still quite limited when compared to the more advanced H100s commonly used in research nowadays. Furthermore, the memory overhead due to processing and storing the KV cache and representative tokens for each memory unit for very long sequence lengths means that we have had to make some specific adjustments in order to ensure that we can efficiently run such experiments on older and limited hardware.

C.2.1 WALL CLOCK TIME

As can be observed in Table 10, the largest increase to wall clock time in our framework is due to the similarity adjustment step. We would also like to note that such times increase steadily as

	InfLLM	EM-LLM			
		S	**S+C**	**SM**	**SM+C**
Time	1.40s	1.57s	1.57s	2.27s	2.27s
Ratio	1.0	1.12	1.12	1.62	1.62

Table 10: Difference in wall-clock time to process a single chunk of 512 tokens for various ablations of our framework as compared to InfLLM. Measured using Mistral-7B (4K+2K) and averaged over the first 100 chunks (51.2K tokens) of a long sequence.

sequence length increases, due to the increasing number of representative tokens involved in the k-NN calculation used for block retrieval, regardless of which method is used.

C.2.2 MEMORY REQUIREMENTS

Seq. Length	KV Cache	Rep. Tokens (max)
20K	9.8GB	0.6GB
1M	488.3GB	30.5GB

Table 11: Memory requirements for components of our framework which scale with sequence length, for a model with 32 layers and 32 KV heads, assuming half float precision and a batch size of 1. The number of representative tokens saved depends on the number of blocks, hence we show the maximum amount of memory required in the event the model segments the sequence into the maximum possible number of blocks.

As shown in Table 11, the KV cache can take up a lot of memory for longer sequences. While the bulk of it is kept on CPU memory until it is needed, such a resource is quickly spent when running multiple instances in parallel on a single node. Likewise, while the representative tokens for each block take up only a fraction of the memory compared to the KV cache, it can quickly become too large to keep on GPU memory. In order to address both of these issues and facilitate the use of our framework on lower-spec hardware, we have introduced various forms of offloading and model parallelisation.

CPU and Disk Offloading

InfLLM already provides details of their least recently used (LRU) KV cache management strategy used to efficiently offload the least-used memory units from GPU to CPU memory. We take inspiration from such a strategy and extend it to use allocated memory slots in CPU memory and dynamically offload such LRU units to disk space when the number of available slots runs low. Allocating and overwriting the memory slots, as is also done in the GPU cache, prevents our process from hanging on the memory which has been freed, avoiding system fragmentation and allocation errors. Furthermore, the ability to offload to disk means that our framework only requires approximately 2GB of CPU memory per instance in order to run with little overhead, as long as there is enough available disk space on the local machine.

Furthermore, we implemented the option to offload representative tokens to CPU memory for very long sequences (1M+), although we note that this further increases the overhead seen in wall clock time during k-NN retrieval.

Model Parallelisation

For very long sequences (2.5M+) it may be more time-efficient to parallelise the model's layers across multiple GPUs in order to keep representative tokens on the same GPU and speed up k-NN retrieval. We used Hugging Face's Accelerate to do this, along with some explicit casting of shared modules. Given a single node with a set number of GPUs and sequence length below 1M tokens, it is faster to offload the representative tokens and run a separate instance on each GPU, than to parallelise on 2 GPUs.

D FURTHER ABLATIONS

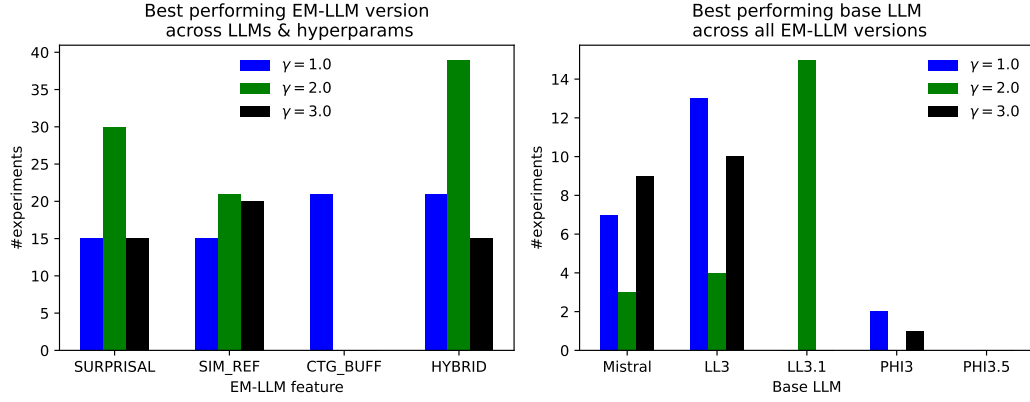## D.1 SURPRISE, REFINEMENT AND CONTIGUITY

Figure 9: (left) Best performing version of the EM-LLM model across base language models (LMs) and hyper-parameters, including the parameter γ that controls the sensitivity of the segmentation threshold in Equation (1). (right) Best performing base LM across all experiments presented in this work.
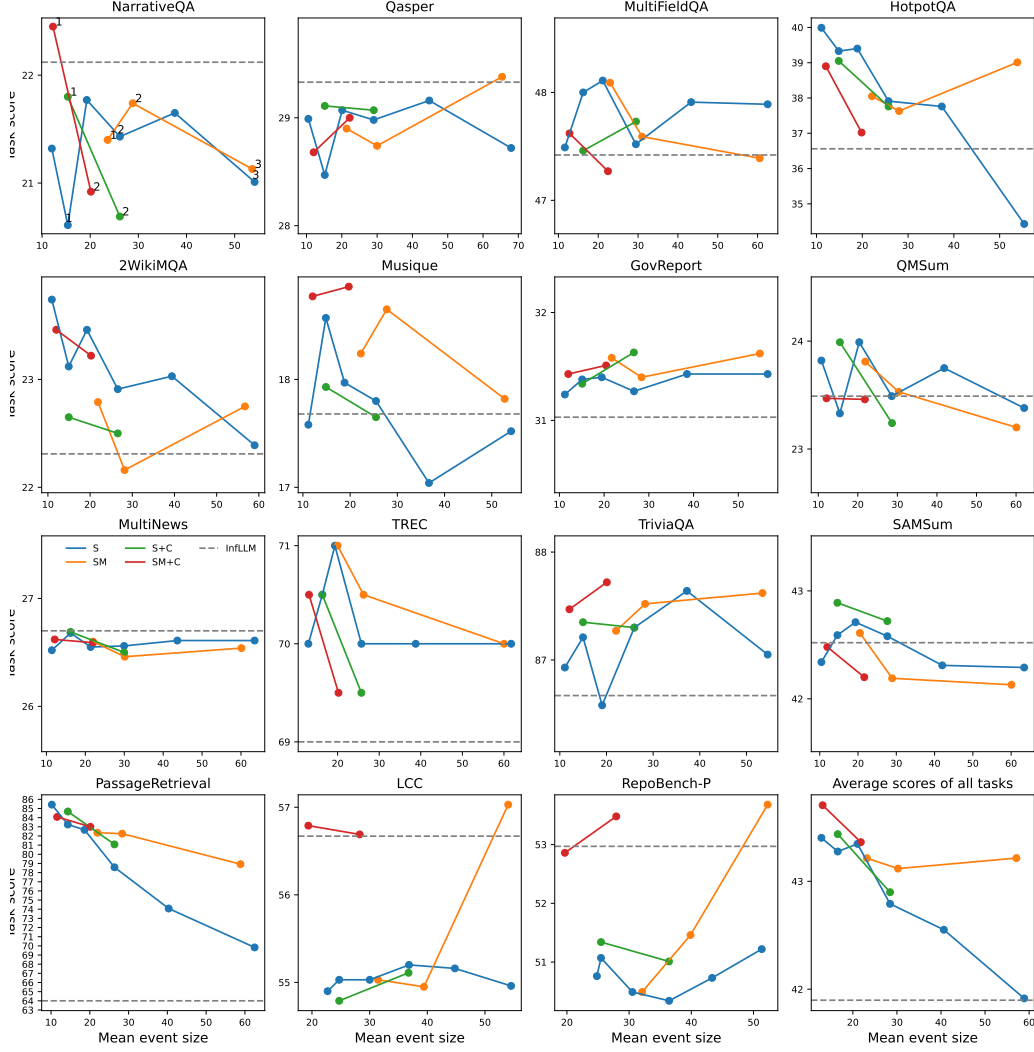
Figure 10: Ablation study in LongBench with Mistral-7B-Instruct-v0.2. Comparison of EM-LLM performance for different combinations of model features (represented by different colours) and different values of γ (the threshold's scaling factor). Model variants are aligned on the x-axis based on the average number of block size that emerges for each case. The γ values for each model variant are shown in the first sub-plot. The corresponding InfLLM performance is also shown.
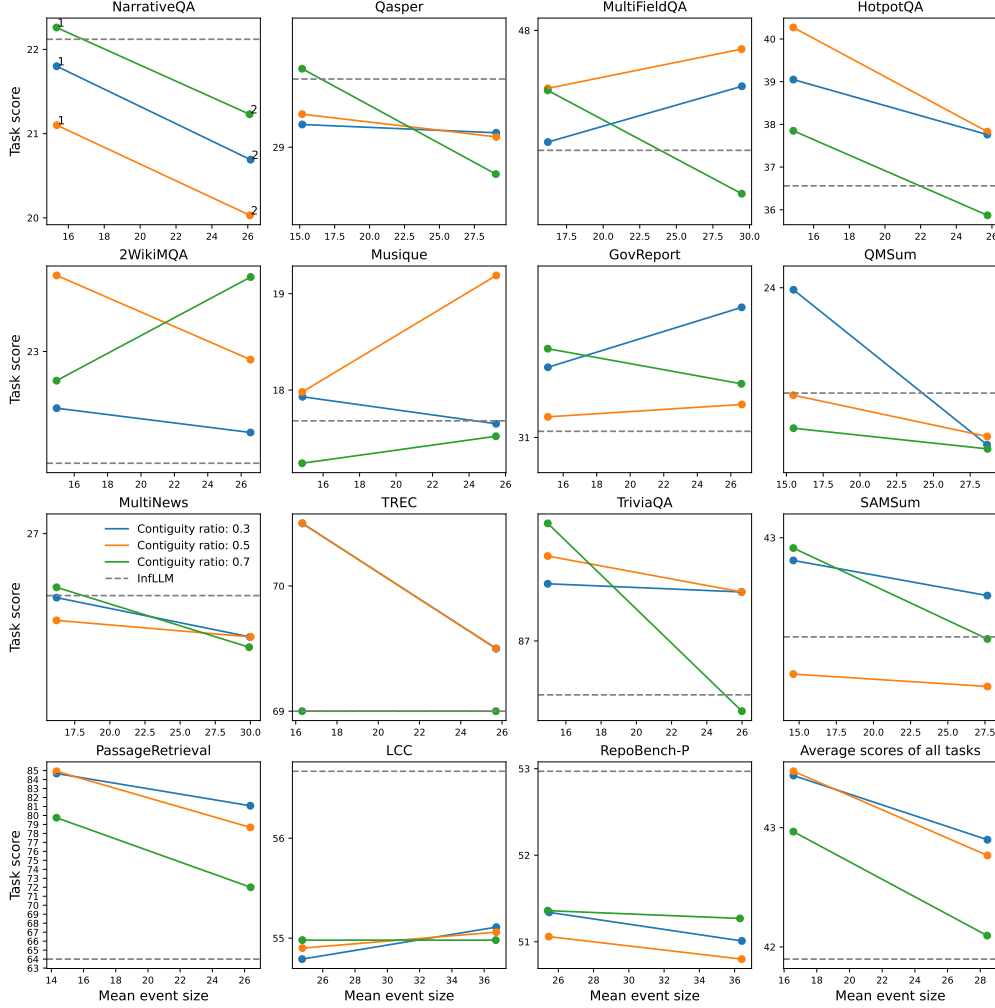
Figure 11: Ablation study in LongBench with Mistral-7B-Instruct-v0.2. Comparison of EM-LLM performance for different ratios of the contiguity and similarity buffers (represented by different colours) and different values of γ. Model variants are aligned on the x-axis based on the average number of block size that emerges for each case. The γ values for each model variant are shown in the first sub-plot. The corresponding InfLLM performance is also shown.

E PROOFS

E.1 APPROXIMATE EQUIVALENCE OF K-NEAREST NEIGHBOURS AND SOFTMAX ATTENTION

Here we will attempt to show that using a k-NN retrieval in a key-value cache as part of the attention mechanism in transformers is an approximation of applying softmax attention over the entire sequence of tokens.

Let q be a query vector and $K = \{k_1, k_2, \ldots, k_n\}$ the set of key vectors in a transformer model with dimensionality d. Each key k_i has a corresponding value vector v_i, with $V = \{v_1, v_2, \ldots, v_n\}$. The softmax attention weights a_i are defined as:

$$a_i = \frac{\exp(q \cdot k_i \, d^{-\frac{1}{2}})}{\sum_{j=1}^{n} \exp(q \cdot k_j \, d^{-\frac{1}{2}})} \tag{6}$$

The output vector u is computed as:

$$u = \sum_{i=1}^{n} a_i v_i \tag{7}$$

In the k-NN approach, a subset K' of size k is selected, containing keys nearest to q. The approximated attention weights a'_i over this subset are:

$$a'_i = \frac{\exp(q \cdot k_i \, d^{-\frac{1}{2}})}{\sum_{j \in K'} \exp(q \cdot k_j \, d^{-\frac{1}{2}})} \quad \text{for } k_i \in K' \tag{8}$$

The approximate output vector u' is:

$$u' = \sum_{k_i \in K'} a'_i v_i \tag{9}$$

ASSUMPTIONS

1. *Exponential Dominance*: The exponential function in the softmax is sharply peaked, implying that keys with the highest similarities to q contribute significantly more to the sum than others.

2. *Representativeness of k-NN Subset*: The subset K' captures the majority of the attention weight from the full set K.

Lemma 1: Dominance of k-NN Subset   If K' consists of the k keys with the highest dot products $q \cdot k_i$, then:

$$\sum_{j \in K'} \exp(q \cdot k_j \, d^{-\frac{1}{2}}) \geq \alpha \sum_{j=1}^{n} \exp(q \cdot k_j \, d^{-\frac{1}{2}}) \tag{10}$$

for some $\alpha \approx 1$, typically very close to 1.

Proof: This follows from the exponential dominance assumption and the nature of the exponential function, which is sharply peaked.

Lemma 2: Approximation of Output Vector   Given the dominance of K' as shown in Lemma 1, the approximate output u' effectively represents the full output u:

$$\|u' - u\| \leq \epsilon \tag{11}$$

where ϵ is a small error term.

Proof: Follows from the weighted sum structure of u and u', using the bounds established in Lemma 1.

Given the lemmas and under the stated assumptions, the k-NN retrieval mechanism within a key-value cache effectively approximates the softmax attention mechanism in transformers. This proof highlights the efficiency versus accuracy trade-off inherent in using approximate methods like k-NN retrieval.